

## INTRODUCTION

Tumor progression is governed not only by the genetic changes intrinsic to cancer cells, but also by epigenetic and environmental factors. Therefore, neoplastic cell factors and biophylactic side factors such as immune reactions are interacting in the survival and development of micrometastasis. Increasing evidence gleaned from studies in immune-compromised hosts suggests that the cellular mechanisms of immunosurveillance influence tumor development. There are several lines of research which indicate the critical role of the immune system in controlling the growth of malignant cells<sup>[1-5]</sup>. Thus, impairment of anti-tumor immunity, which leads to immunologic toleration of malignant cells, contributes to the development and progression of peritoneal metastasis<sup>[6]</sup>. The elimination phase of the cancer immunosurveillance mechanism is thought to be a continuous process, and local control of metastatic invasion by the immune system may be critical for survival. However, the role of lymphocytes in the peritoneal cavity for anti-tumor immunity in gastric cancer patients is unknown<sup>[7]</sup>.

Studies in rodents have demonstrated that adoptive immunotherapy with antigen-specific CD8<sup>+</sup> T cells is effective for cancer, and there is evidence that this approach has therapeutic activity in humans<sup>[8-10]</sup>. Memory T cells circulate throughout all tissues of the body and are primed to rapidly produce secondary immune responses upon antigen challenge<sup>[11]</sup>. The nature of the cells that mediate the different facts of immunological memory remains unresolved. Natural killer T cells are a specialized subset of T cells. They express T-cell and natural killer-lineage cell surface markers and key cytokines, which regulate the course of the immune response. There are many mechanisms that regulate and dampen the immune response to cancers<sup>[12,15]</sup>. Regulatory T cells protect the host from autoimmune disease by suppressing self-reactive immune cells. As such, regulatory T cells may also block antitumor immune responses. Regulatory T cells have been an active research area in basic as well as in clinical immunology<sup>[16-18]</sup>. Th1 immune responses are considered to be essential for eradicating malignant cells. Based on the cytokine profile, interferon-gamma is a Th1 cytokine with an antitumor effect. Interleukin-10, a Th2 cytokine, inhibits Th1 immune responses and enhances the production of other Th2 cytokines<sup>[19,22]</sup>.

In order to clarify the clinical significance of the host immune response within the peritoneal cavity in patients with gastric cancer, we conducted an immunological analysis of the peritoneal lavage obtained from patients at the time of gastrectomy.

## MATERIALS AND METHODS

### Patients

A total of 75 patients (50 males and 25 females; mean age: 64.3 years) were included in this study. Sixty-four patients were histologically diagnosed as having gastric cancer. Among these, 56 had gastrectomy, 2 underwent bypass op-

**Table 1 Clinicopathological features in the examined gastric cancer patients**

| Variables               | No. of patients |
|-------------------------|-----------------|
| Total cases             | 64              |
| Age (yr)                | 67.5 ± 2.8      |
| Sex (male/female)       | 42/22           |
| Depth of tumor invasion |                 |
| T1                      | 32              |
| T2                      | 20              |
| T3                      | 9               |
| T4                      | 3               |
| Lymphnode metastasis    |                 |
| N0                      | 34              |
| N1                      | 12              |
| N2                      | 14              |
| N3                      | 4               |
| Peritoneal metastasis   |                 |
| Absent                  | 56              |
| Present                 | 8               |
| Cytology                |                 |
| Negative                | 57              |
| Positive                | 7               |
| Stage                   |                 |
| Stage I A               | 25              |
| Stage I B               | 13              |
| Stage II                | 7               |
| Stage III               | 7               |
| Stage IV                | 12              |

eration, and 6 had exploratory laparotomy. Eleven patients who underwent laparoscopic cholecystectomy for benign disease acted as controls. The resected specimens were histologically examined by hematoxylin and eosin staining according to the general rules of the Japanese Classification of Gastric Carcinoma<sup>[23]</sup>. The investigation protocol was approved by the Institutional Review Board of the Nagasaki University School of Medicine (#14122694). Written informed consent was obtained from all patients. The stages of gastric cancer patients were as follows: stage I A, *n* = 25 patients; stage I B, *n* = 13; stage II, *n* = 7; stage III, *n* = 7; and stage IV, *n* = 12. The clinicopathological features of the patients are shown in Table 1.

### Isolation of mononuclear cells from peripheral blood and peritoneal lavage

Endotracheal general anesthesia was induced and 10 mL of peripheral blood was taken from all patients. Four hundred milliliter of physiological saline was poured into the peritoneal cavity prior to manipulation of the tumor, and was recovered after being gently stirred. Half of the peritoneal lavage was allocated for conventional cytology and carcinoembryonic antigen (CEA) analysis by an enzyme-linked immunosorbent assay. The other half of the peritoneal lavage was immediately centrifuged at 2000 rpm for 10 min, and the supernatants were assayed for CEA values. The peritoneal CEA levels were then measured using an enzyme immunoassay kit (IMx-SERECT CEA, Dainabot, Tokyo) and the protein concentration was determined using a protein assay kit (Bio-Rad, Richmond, CA, United States). The cell component was used for lymphocyte analysis. Lymphocytes from peripheral

Table 2 Carcinoembryonic antigen values in sera and peritoneal lavage

| Source                                 | Control             | Stage I A           | Stage I B            | Stage II            | Stage III            | Stage IV                |
|--|---------------------|---------------------|----------------------|---------------------|----------------------|-------------------------|
| CEA                                    |                     |                     |                      |                     |                      |                         |
| PB (ng/mL)                             | Not tested          | 2.09 (1.39-2.78)    | 2.03 (0.96-3.1)      | 3.06 (2.04-4.07)    | 2.54 (0.38-4.69)     | 7.98 (1.18-15.82)       |
| PL (ng/g protein)                      | 56.53 (21.82-91.24) | 44.17 (27.37-60.96) | 61.95 (11.98-111.91) | 83.14 (7.31-187.54) | 262.63 (7.26-517.26) | 1234.00 (87.77-2380.22) |
| CD4/CD8                                |                     |                     |                      |                     |                      |                         |
| PB (ratio)                             | 5.379 (2.705-8.052) | 5.595 (3.224-7.967) | 4.571 (2.057-7.086)  | 5.277 (1.369-9.184) | 7.999 (3.366-12.632) | 4.156 (2.228-6.083)     |
| PL (ratio)                             | 0.494 (0.338-0.649) | 0.553 (0.421-0.685) | 0.697 (0.511-0.883)  | 0.638 (0.395-0.881) | 1.242 (0.961-1.522)  | 1.158 (0.907-1.408)     |
| CD45RA <sup>+</sup> /CCR7 <sup>-</sup> |                     |                     |                      |                     |                      |                         |
| PB (%)                                 | 60.43 (46.42-74.44) | 58.29 (48.93-67.64) | 53.92 (32.65-75.2)   | 57.36 (42.01-72.71) | 49.01 (29.31-68.71)  | 45.73 (32.79-58.67)     |
| PL (%)                                 | 81.17 (81.12-93.22) | 81.67 (76.35-87.01) | 76.2 (59.43-92.96)   | 72.3 (61.01-83.58)  | 68.36 (58.70-78.02)  | 51.92 (38.34-65.50)     |
| NKT                                    |                     |                     |                      |                     |                      |                         |
| PB (%)                                 | 9.19 (5.83-12.54)   | 7.59 (5.63-9.56)    | 9.47 (4.41-14.53)    | 10.71 (1.55-19.87)  | 5.43 (0.54-10.33)    | 7.16 (3.95-10.3)        |
| PL (%)                                 | 18.1 (9.83-26.37)   | 17.25 (13.54-20.97) | 15.74 (9.23-22.25)   | 15.38 (7.71-23.04)  | 9.66 (1.2-18.11)     | 9.91 (6.94-12.88)       |

PB: Peripheral blood; PL: Peritoneal lavage; CI: Confidence interval. The data are presented as the median and 95% CI. The statistical analysis of the differences revealed higher CEA and CD4/CD8, lower CD8<sup>+</sup> effector memory T cells and NKT cells in the peritoneal cavity in patients with advanced stage than in controls.

blood were isolated by density centrifugation over Ficoll-Paque<sup>TM</sup> gradients (Amersham, Uppsala, Sweden).

### Flow cytometry

The following monoclonal antibodies were used in the present study: fluorescein isothiocyanate (FITC)-conjugated anti-CD8, FITC-CD25, FITC-CD45RA, phycoerythrin (PE)-conjugated anti-CD4, PE-CD56, PE-CCR7, PE-IFN- $\gamma$ , PE-IL-10, PE-Foxp3, cychrome (Cy)-conjugated anti-CD3, and Cy-CD8 (BD Pharmingen, San Diego, CA, United States). Single-cell suspensions were stained in phosphate-buffered saline-1% fetal calf serum at saturating concentrations according to standard procedures. Flow cytometry was performed on the BD Biosystems-FACSCanto II system (BD Biosciences, San Diego, CA, United States), and FACSDiva software (BD Biosciences, San Diego, CA, United States) was used for analysis. All analyses of T cells were carried out after gating by CD3. The ratio of the percentage of CD4 and CD8 cells was represented as the CD4/CD8 ratio.

### Intracellular staining for Foxp3

Intracellular staining for Foxp3 was performed using the Human Foxp3 Buffer set (BD Pharmingen, San Diego, CA, United States) according to the manufacturer's protocol.

### Cytokine assays

Anti-IFN- $\gamma$ -PE and anti-IL-10-PE mAbs were used for the intracellular analysis of cytokine production. Peripheral and intra-peritoneal lymphocytes were activated with 10 ng/mL phorbol 12-myristate-13-acetate (PMA), 0.5  $\mu$ g/mL Ionomycin, and 1  $\mu$ L/mL GolgiPlug (BD Pharmingen, San Diego, CA, United States) for 4 h. Cells were washed, fixed and permeabilized by Cytofix/Cytoperm solution (BD Pharmingen, San Diego, CA, United States), and stained with titrated amounts of cytokine-specific antibodies.

Next, the CD4<sup>+</sup> CD25<sup>+</sup> T cells were isolated from peripheral blood by magnetic beads (Miltenyi Biotech, BergischGladbach, Germany). These CD4<sup>+</sup> CD25<sup>+</sup> T cells

were mixed with intraperitoneal lymphocytes at a ratio of 1:10 and co-cultivated for 4 d in RPMI with 10% FBS. The CD4<sup>+</sup> CD25<sup>-</sup> T cells were co-cultivated with intraperitoneal lymphocytes as controls. The cytokine assay was performed by the intracellular cytokine method after 4 d of co-cultivation.

### Statistical analysis

The statistical analysis was performed using the Kruskal-Wallis test (non-parametric ANOVA) using a personal computer and the StatViewV.5.0 software package (SAS Institute, Cary, NC, United States). *P* values less than 0.05 were considered to indicate statistical significance.

## RESULTS

### Carcinoembryonic antigen values in sera and peritoneal lavage

For the interaction between peripheral blood and the peritoneal cavity, we investigated the CEA values in both serum and peritoneal lavage at the time of surgery. The serum CEA values were elevated only in patients with stage IV disease. On the other hand, the values in peritoneal lavage were found to be elevated even at stage III, and they were also related to the clinical stage (Table 2).

### Analysis of lymphocyte populations in peripheral blood and the peritoneal cavity

After purification of lymphocytes from peritoneal lavage, we investigated the phenotypes of lymphocytes in the peripheral blood and the peritoneal cavity. The mean value of the CD4/CD8 ratio for all patients was 2.17 in peripheral blood. The CD8<sup>+</sup> T cells were dominant in the peritoneal cavity and the CD4/CD8 ratio was reversed. The ratio in patients with stage III or IV was significantly higher than in stage I or control patients (Table 2).

The CCR7<sup>+</sup> CD45RA<sup>-</sup> CD8<sup>+</sup> T cells were counted as effector memory T cell subsets. The percentage of effector memory T cells in the peritoneal cavity was higher than that in peripheral blood. However, the percentage

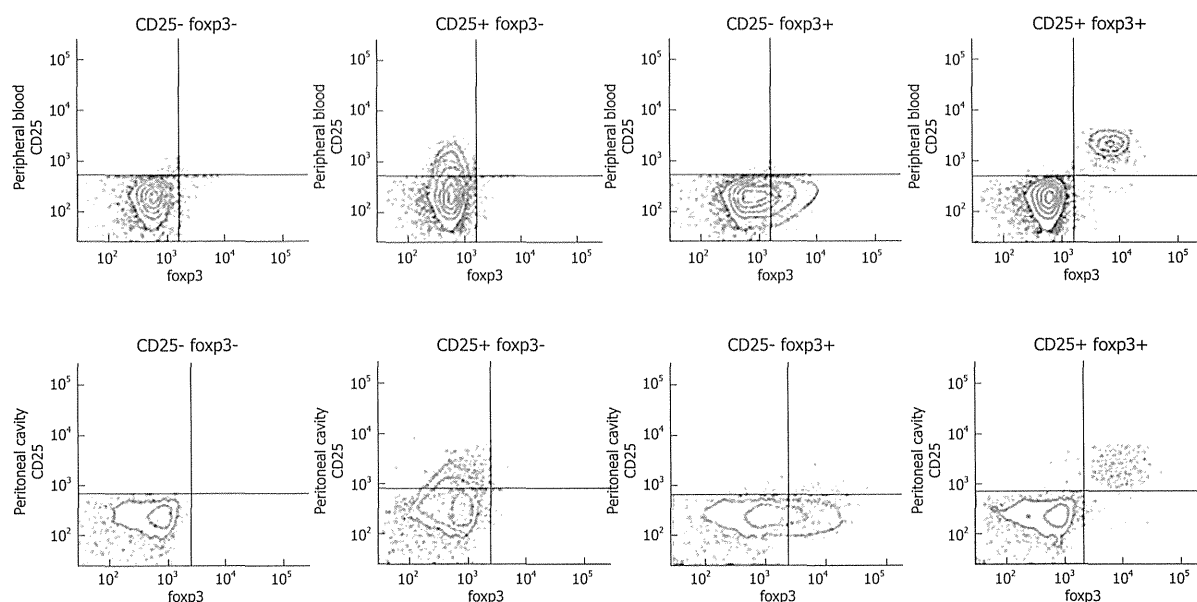


Figure 1 Co-staining with foxp3 and CD25 for CD4<sup>+</sup> T cells. High correlation was shown between both populations.

decreased in association with the clinical stage (Table 2). The CD3<sup>+</sup>CD56<sup>+</sup> cells were measured as natural killer T cells. The percentage of these cells in the peritoneal lavage was also low in patients with stage III or stage IV (Table 2). As the co-staining of foxp3 and CD25 revealed a high correlation between both populations, CD25<sup>high</sup> was used following cytokine producing assays (Figure 1). The frequency of CD4<sup>+</sup> CD25<sup>high</sup> T cells in patients with advanced stage cancer was higher than that in control patients in both peripheral blood and the peritoneal cavity (Figure 2A and B).

#### Cytokine production by lymphocytes

The cytokine production from CD3<sup>+</sup> T cells after stimulation with PMA + ionomycin was evaluated by a cytokine production assay. The lymphocytes in the peritoneal cavity were more sensitive for the production of IFN- $\gamma$  than those in the peripheral blood. The ratio of IFN- $\gamma$  producing cells in the peritoneal cavity was significantly lower in patients with advanced stage disease in comparison to the controls (Figure 3A and B). The ratio of IL-10 producing cells in the peritoneal cavity in patients with advanced stages was higher in comparison to the controls (Figure 3C and D).

#### Cytokine assays of intra-peritoneal lymphocytes after co-cultivation with self- CD4<sup>+</sup> CD25<sup>high</sup> T cells

In order to investigate whether the suppression of IFN- $\gamma$  production from T cells in the peritoneal cavity at advanced stages was caused by CD4<sup>+</sup> CD25<sup>high</sup> T cells, further assays were performed. The IFN- $\gamma$  production of CD8<sup>+</sup> T cells was suppressed in intra-peritoneal lymphocytes co-cultivated with isolated CD4<sup>+</sup> CD25<sup>high</sup> T cells from self-peripheral blood (Figure 4A). No inhibition was seen when the lymphocytes were co-cultivated with CD4<sup>+</sup>

CD25<sup>-</sup> cells (Figure 4B).

## DISCUSSION

The peritoneal cavity is a compartment in which the immunological host-tumor interaction can occur<sup>[24]</sup>. This study investigated lymphocytes in the peritoneal cavity of patients with gastric cancer in relation to anti-tumor immunity. Some tumors can acquire the ability to down-regulate immune responses and exploit this action to promote tumor cell proliferation, survival, and invasion<sup>[10,25]</sup>. Therefore, the presence of leukocytes in the peritoneal cavity may be a consequence of an immune response that favors either dissemination of tumor cells or a protective host response. Malignant ascites has been used as a common source of immunological analysis in previous reports<sup>[11,26]</sup>. To the best of our knowledge, there are no reports describing the lymphocyte and cytokine production ability in peritoneal lavage from patients with gastric cancer at the time of gastrectomy.

In our initial experiments, the CEA values in peritoneal lavage were found to correlate with the clinical stages. Interestingly, the CEA values were elevated even in cases without serosal invasion. This result suggests that some fragments of cancer cells may spread throughout the peritoneal cavity and induce an immune reaction between the tumor and host<sup>[26,27]</sup>.

The frequency of CD4<sup>+</sup> T cells in all patients was higher than that of CD8<sup>+</sup> T cells in peripheral blood, but this pattern was reversed in peritoneal lavage fluid. CD8<sup>+</sup> T cells were dominant in the peritoneal cavity. Our data suggested that the immunological environment in the peripheral blood is different from that in the peritoneal cavity. There were significant differences in the CD4/CD8 ratio in the peritoneal cavity between gastric cancer

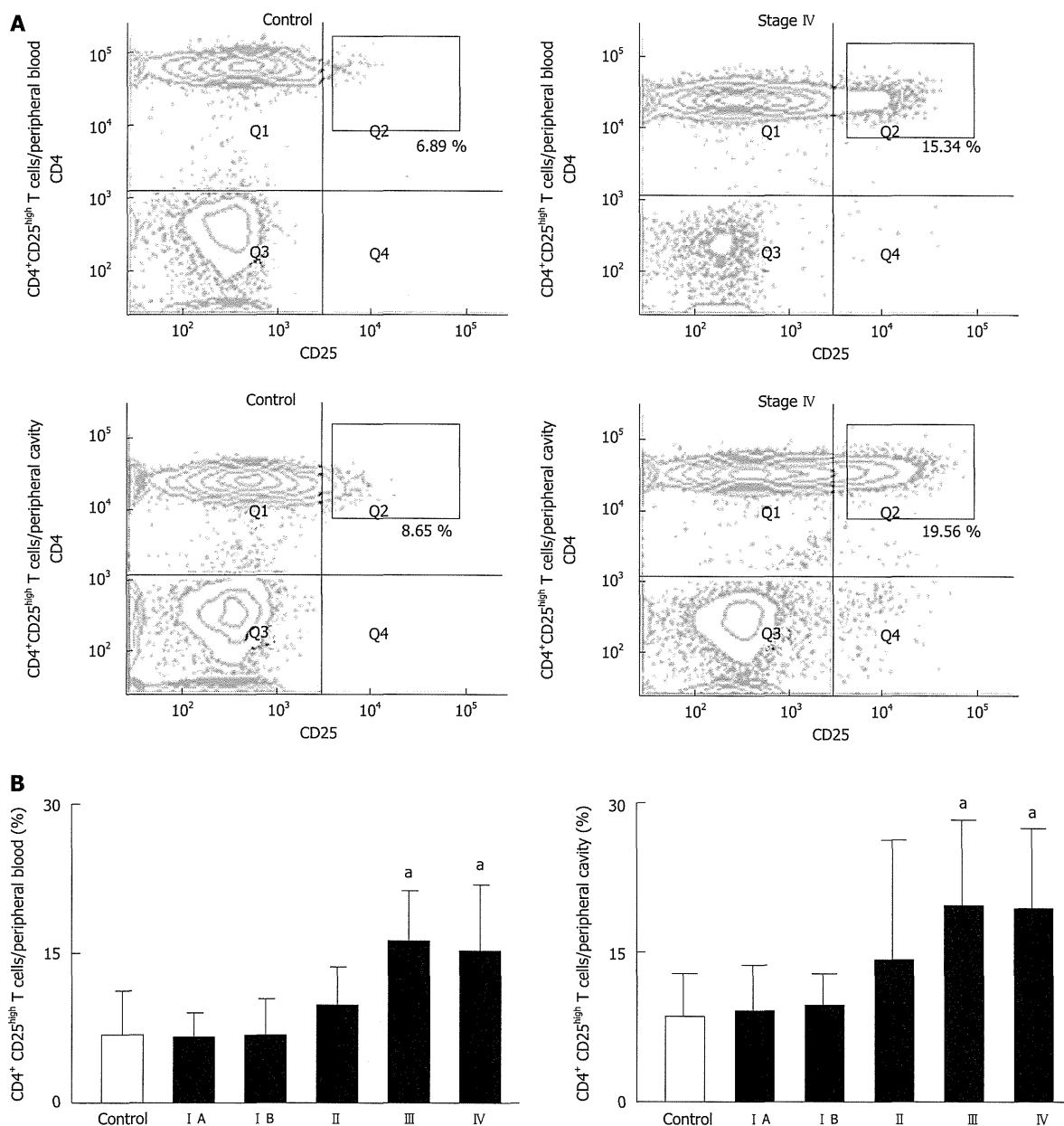


**Figure 2** Analysis of lymphocyte populations in peripheral blood and the peritoneal cavity. A: The gating and counting of CD4<sup>+</sup> CD25<sup>high</sup> T cell population by flow cytometry; B: The percentage of CD4<sup>+</sup> CD25<sup>high</sup> T cells in the CD4<sup>+</sup> T cell population in peripheral blood and peritoneal lavage of patients at each stage of gastric cancer and control patients. Data are presented as the mean ± SD.

patients at advanced stage and control patients. Cancer progression may have an effect on the balance of the T cell population in the peritoneal cavity.

Immunological memory is demonstrated by following T cell subsets: lymph-node-homing cells lacking inflammatory and cytotoxic function (defined as central memory T cells, CCR7<sup>+</sup> CD45RA<sup>-</sup>) and tissue-homing cells endowed with various effector functions (defined as effector memory T cells, CCR7<sup>-</sup> CD45RA<sup>+</sup>). These two subsets allow for the division of labor among memory cells. Effector memory T cells represent a readily available pool of antigen-primed cells that can enter peripheral tissues

to mediate inflammatory reactions or cytotoxicity, thus rapidly containing invasive pathogens and cancer antigens<sup>[11,28-31]</sup>. Our data show that CD8<sup>+</sup> effector memory T cells were rich in the peritoneal cavity. This indicates the migration of effector memory cells from the peripheral blood to local sites. However, in advanced cases, the frequency of CD8<sup>+</sup> effector memory cells in the peritoneal lavage was low. These results suggest that the peritoneal cavity exerts the local immune response, more than peripheral blood.

Natural killer T cells, a unique lymphocyte subpopulation, are characterized by the expression of invariant an-

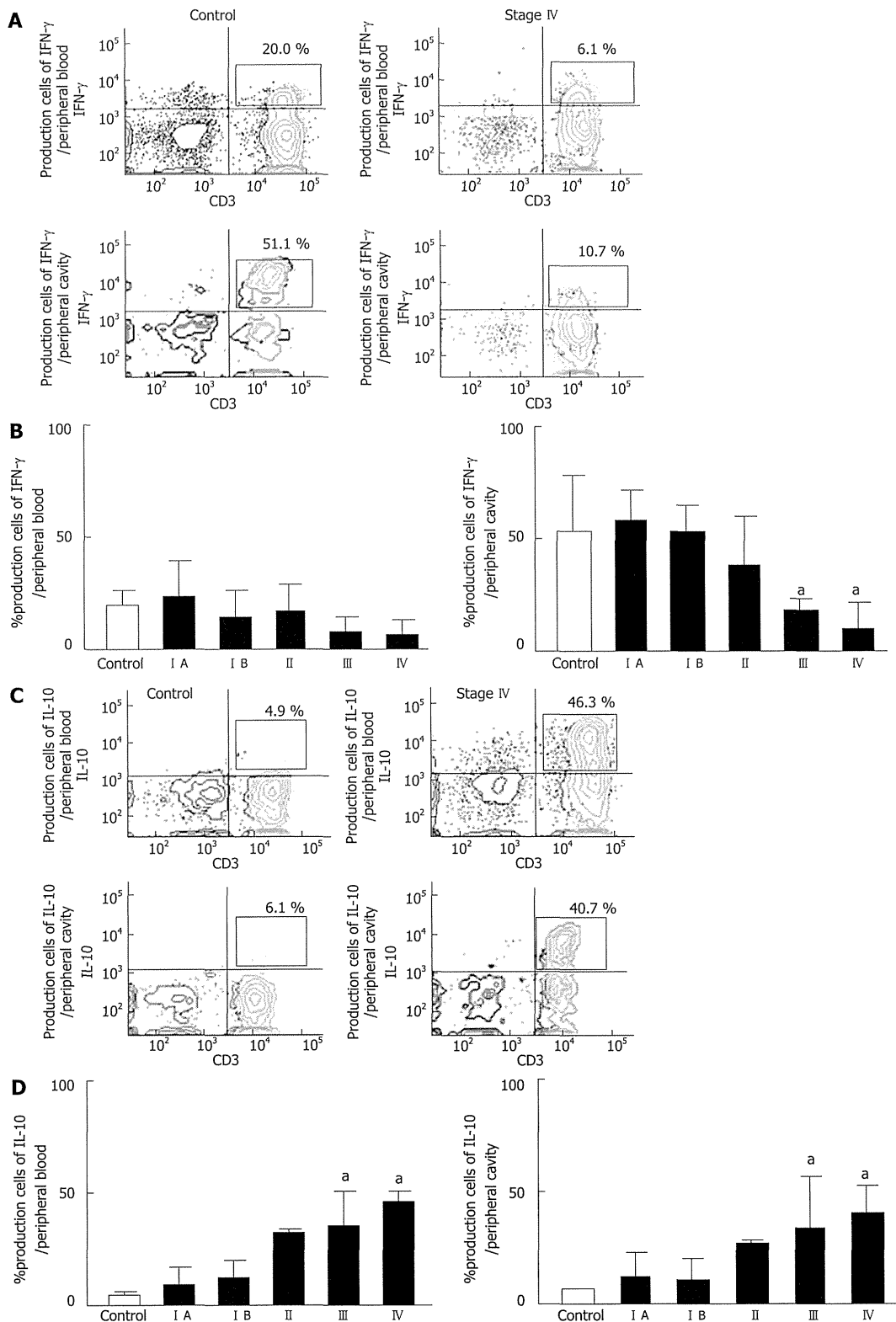


**Figure 3** Cytokine production by lymphocytes. **A:** The gating and counting of the IFN- $\gamma$  producing cell population by flow cytometry; **B:** The percentage of IFN- $\gamma$  producing cells in the CD3<sup>+</sup> cell population stimulated with PMA + ionomycin in peripheral blood and peritoneal lavage of patients at each stage of gastric cancer and control patients. Data are presented as the mean  $\pm$  SD. The statistical analysis was performed by the Kruskal-Wallis test. After gating of CD3<sup>+</sup> T cells, 10 000 events were analyzed. The production of IFN- $\gamma$  in the peritoneal cavity was higher than that in the peripheral blood. The ratio of IFN- $\gamma$  production cells in the peritoneal lavage was significantly lower in patients with advanced-stage than in controls [control vs stage IV: 51.1 (35.1-67.1) vs 10.7 (2.6-22.1), <sup>a</sup> $P < 0.05$ ]; **C:** The gating and counting of the IL-10 producing cell population by flow cytometry; **D:** The percentage of IL-10 producing cells in the CD3<sup>+</sup> cells stimulated with PMA + ionomycin in peripheral blood and peritoneal lavage of patients at each stage of gastric cancer and control patients. Data are presented as the mean  $\pm$  SD. The ratio of IL-10 producing cells in peripheral blood and intra-peritoneal lymphocytes was significantly higher in patients at advanced stage than in controls [control vs stage IV: 6.1 (3.94-8.25) vs 40.7 (18.35-63.0), <sup>a</sup> $P < 0.05$ ].

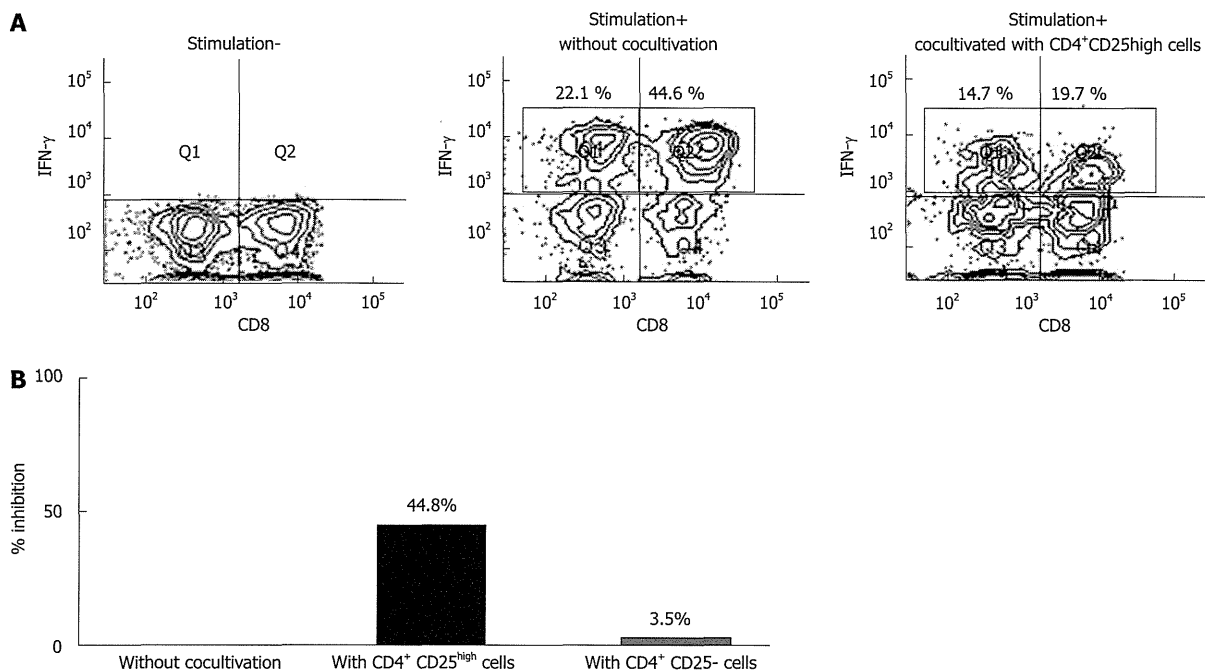


**Figure 4** Cytokine assays of intra-peritoneal lymphocytes after co-cultivation with self-CD4<sup>+</sup>CD25<sup>high</sup>T cells. A: IFN- $\gamma$  production in intra-peritoneal lymphocytes co-cultivated with self- CD4<sup>+</sup> CD25<sup>high</sup> T cells; B: Either CD4<sup>+</sup> CD25<sup>high</sup> T cells or CD4<sup>+</sup> CD25<sup>-</sup> T cells.

tigen receptors<sup>[12,13]</sup>. Natural killer T cells have been suggested to serve as a bridge between innate and acquired immunity<sup>[14,15]</sup>. However, the mechanisms underlying the anti-tumor effect of human natural killer T cell-mediated immunotherapy remain unclear so far. The frequency of natural killer T cells was lower in patients with stages III and IV than in control patients. Therefore, a decrease in the number of natural killer T cells in the peritoneal cavity may be one aspect of the interaction between host-immunity and cancer progression.

Recent studies have shown that CD4<sup>+</sup> CD25<sup>high</sup> foxp3<sup>+</sup> T cells exhibiting regulatory/suppressive properties are naturally present in humans<sup>[16-18]</sup>. The roles of regulatory T cells have been active topics of research in both basic and clinical immunology. Naturally-occurring regulatory T cells represent a small fraction (5%-6%) of the overall CD4<sup>+</sup> T cell population, and play an important role in down-regulation of the response of T cells to foreign and self antigens<sup>[31]</sup>. The depletion of this subset of regulatory T cells in normal hosts results in various autoimmune diseases because the host immune system is unchecked and attacks the body's own tissues<sup>[28]</sup>. Despite the importance of these cells in preventing autoimmune disease, their presence in the tumor microenvironment diminishes anti-tumor immune responses<sup>[32-36]</sup>.

Within the CD4<sup>+</sup> T cell subset, there is a population of naturally occurring foxp3<sup>+</sup> T cells that are defined as regulatory T cells. These cells can be identified as CD4<sup>+</sup>foxp3<sup>+</sup> T cells by flow cytometry. However, because foxp3 is intracellular and requires permeabilization of cells for detection by flow cytometry, regulatory T cells are isolated as CD4<sup>+</sup>CD25<sup>high</sup> T cells, which were shown to

have functional suppressive abilities in our co-culture experiments<sup>[37]</sup>. In the present study, the mean percentage of CD4<sup>+</sup> CD25<sup>high</sup> T cells in the peritoneal cavity in advanced gastric cancer patients was higher than that of control patients. After the co-cultivation of the self-CD4<sup>+</sup> CD25<sup>high</sup> T cell population of intra-peritoneal lymphocytes, the production of IFN- $\gamma$  was inhibited.

IFN- $\gamma$ , a Th1 cytokine, not only exerts an anti-tumor effect, but also inhibits the proliferation of Th2 clones<sup>[19,20]</sup>. IL-10, a Th2 cytokine, suppresses the synthesis of Th1 cytokines such as IFN- $\gamma$ <sup>[21,22]</sup>. This study showed that the production of intracellular cytokines in the peritoneal cavity was higher than that in the peripheral blood after appropriate stimulation. IFN- $\gamma$  production was down-regulated in advanced cases, but not in the controls and stage I patients. On the other hand, IL-10 production was up-regulated, which revealed the switch of Th1 and Th2 responses in the peritoneal cavity of these patients. IFN- $\gamma$  production in intra-peritoneal lymphocytes was suppressed after co-cultivation with self-CD4<sup>+</sup> CD25<sup>high</sup> T cells, but not CD4<sup>+</sup> CD25<sup>-</sup> T cells. Interestingly, the replacement of CD4<sup>+</sup> CD25<sup>-</sup> T cells for CD4<sup>+</sup> CD25<sup>high</sup> T cells could recover the production of IFN- $\gamma$  in intra-peritoneal lymphocytes.

## COMMENTS

### Background

The peritoneal cavity is a compartment in which immunological host-tumor interactions can occur. Neoplastic cell factors and biophylactic side factors such as immune reactions are interacting in the survival and development of micro-metastasis. However, the role of lymphocytes in the peritoneal cavity of gastric cancer patients is unclear.

### Research frontiers

Clinical and experimental studies have established that leukocyte infiltrations around tumors promote the development or regression of solid tumors, but whether the organ-specific cellular and molecular programs promote tumor growth or exhibit anti-tumor immunity by leukocytes are incompletely understood. Recent studies have shown that CD4<sup>+</sup> CD25<sup>high</sup> foxp3<sup>+</sup> T cells exhibiting regulatory/suppressive properties are naturally present in humans. The roles of regulatory T cells have been active topics of research in both basic and clinical immunology.

### Innovations and breakthroughs

In most previous studies, malignant ascites have been a common source of immunological analysis. However, there are no reports describing the lymphocyte and cytokine production ability in peritoneal lavage from patients with gastric cancer at the time of gastrectomy. In the present study, CD4<sup>+</sup> CD25<sup>high</sup> T cells were found to be increased in the peritoneal cavity of advanced gastric cancer patients, but in the co-cultivation of the self- CD4<sup>+</sup> CD25<sup>high</sup> T cell population of intra-peritoneal lymphocytes, the production of IFN- $\gamma$  was inhibited.

### Applications

Peritoneal lavage samples from patients with gastric cancer are more susceptible than peripheral blood for monitoring the interaction between the host's immune system and tumor cells.

### Terminology

Regulatory T cells: Regulatory T cells contribute to the maintenance of immunologic self-tolerance. Recent reports underscore that regulatory T cells not only play a role in the maintenance of immunotolerance but are also potent inhibitors of antitumor immune responses.

### Peer review

The authors have investigated T-cells isolated from peripheral blood and peritoneal lavage in patients with gastric cancer and controls. Main findings are that in stage III and IV gastric cancers the lavage fluid contains less CD8 memory cells, NKT cells and more CD25<sup>high</sup> regulatory T cells.

## REFERENCES

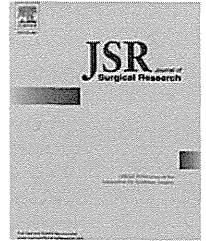
- Huber V, Fais S, Iero M, Lugini L, Canese P, Squarcina P, Zaccheddu A, Colone M, Arancia G, Gentile M, Seregini E, Valenti R, Ballabio G, Belli F, Leo E, Parmiani G, Rivoltini L. Human colorectal cancer cells induce T-cell death through release of proapoptotic microvesicles: role in immune escape. *Gastroenterology* 2005; **128**: 1796-1804
- Galon J, Costes A, Sanchez-Cabo F, Kirilovsky A, Mlecnik B, Lagorce-Pagès C, Tosolini M, Camus M, Berger A, Wind P, Zinzindohoué F, Bruneval P, Cugnenc PH, Trajanoski Z, Fridman WH, Pagès F. Type, density, and location of immune cells within human colorectal tumors predict clinical outcome. *Science* 2006; **313**: 1960-1964
- Susumu S, Nagata Y, Ito S, Matsuo M, Valmori D, Yui K, Udono H, Kanematsu T. Cross-presentation of NY-ESO-1 cytotoxic T lymphocyte epitope fused to human heat shock cognate protein 70 by dendritic cells. *Cancer Sci* 2008; **99**: 107-112
- Koizumi K, Hojo S, Akashi T, Yasumoto K, Saiki I. Chemokine receptors in cancer metastasis and cancer cell-derived chemokines in host immune response. *Cancer Sci* 2007; **98**: 1652-1658
- Tsujimoto H, Ono S, Ichikura T, Matsumoto Y, Yamamoto J, Hase K. Roles of inflammatory cytokines in the progression of gastric cancer: friends or foes? *Gastric Cancer* 2010; **13**: 212-221
- Nan KJ, Wei YC, Zhou FL, Li CL, Sui CG, Hui LY, Gao CG. Effects of depression on parameters of cell-mediated immunity in patients with digestive tract cancers. *World J Gastroenterol* 2004; **10**: 268-272
- Atanackovic D, Block A, de Weerth A, Faltz C, Hossfeld DK, Hegewisch-Becker S. Characterization of effusion-infiltrating T cells: benign versus malignant effusions. *Clin Cancer Res* 2004; **10**: 2600-2608
- Cheever MA, Greenberg PD, Fefer A. Specificity of adoptive chemoimmunotherapy of established syngeneic tumors. *J Immunol* 1980; **125**: 711-714
- Dudley ME, Wunderlich JR, Robbins PF, Yang JC, Hwu P, Schwartzentruber DJ, Topalian SL, Sherry R, Restifo NP, Hübicki AM, Robinson MR, Raffeld M, Duray P, Seipp CA, Rogers-Freezer L, Morton KE, Mavroukakis SA, White DE, Rosenberg SA. Cancer regression and autoimmunity in patients after clonal repopulation with antitumor lymphocytes. *Science* 2002; **298**: 850-854
- Dudley ME, Wunderlich JR, Yang JC, Sherry RM, Topalian SL, Restifo NP, Royal RE, Kammula U, White DE, Mavroukakis SA, Rogers LJ, Gracia GJ, Jones SA, Mungameli DP, Pelletier MM, Gea-Banacloche J, Robinson MR, Berman DM, Filie AC, Abati A, Rosenberg SA. Adoptive cell transfer therapy following non-myeloablative but lymphodepleting chemotherapy for the treatment of patients with refractory metastatic melanoma. *J Clin Oncol* 2005; **23**: 2346-2357
- Sallusto F, Lenig D, Förster R, Lipp M, Lanzavecchia A. Two subsets of memory T lymphocytes with distinct homing potentials and effector functions. *Nature* 1999; **401**: 708-712
- Taniguchi M, Harada M, Kojo S, Nakayama T, Wakao H. The regulatory role of Valpha14 NKT cells in innate and acquired immune response. *Annu Rev Immunol* 2003; **21**: 483-513
- Brigl M, Brenner MB. CD1: antigen presentation and T cell function. *Annu Rev Immunol* 2004; **22**: 817-890
- Taniguchi M, Seino K, Nakayama T. The NKT cell system: bridging innate and acquired immunity. *Nat Immunol* 2003; **4**: 1164-1165
- Motohashi S, Nakayama T. Clinical applications of natural killer T cell-based immunotherapy for cancer. *Cancer Sci* 2008; **99**: 638-645
- Sakaguchi S. Naturally arising CD4<sup>+</sup> regulatory t cells for immunologic self-tolerance and negative control of immune responses. *Annu Rev Immunol* 2004; **22**: 531-562
- Linehan DC, Goedegebuure PS. CD25<sup>+</sup> CD4<sup>+</sup> regulatory T-cells in cancer. *Immunol Res* 2005; **32**: 155-168
- Imai H, Saio M, Nonaka K, Suwa T, Umemura N, Ouyang GF, Nakagawa J, Tomita H, Osada S, Sugiyama Y, Adachi Y, Takami T. Depletion of CD4<sup>+</sup>CD25<sup>+</sup> regulatory T cells enhances interleukin-2-induced antitumor immunity in a mouse model of colon adenocarcinoma. *Cancer Sci* 2007; **98**: 416-423
- Fernandez-Botran R, Sanders VM, Mosmann TR, Vitetta ES. Lymphokine-mediated regulation of the proliferative response of clones of T helper 1 and T helper 2 cells. *J Exp Med* 1988; **168**: 543-558
- Rayman P, Wesa AK, Richmond AL, Das T, Biswas K, Raval G, Storkus WJ, Tannenbaum C, Novick A, Bukowski R, Finke J. Effect of renal cell carcinomas on the development of type 1 T-cell responses. *Clin Cancer Res* 2004; **10**: 6360S-6366S
- Fiorentino DF, Zlotnik A, Vieira P, Mosmann TR, Howard M, Moore KW, O'Garra A. IL-10 acts on the antigen-presenting cell to inhibit cytokine production by Th1 cells. *J Immunol* 1991; **146**: 3444-3451
- Bai XF, Zhu J, Zhang GX, Kaponides G, Höjeberg B, van der Meide PH, Link H. IL-10 suppresses experimental autoimmune neuritis and down-regulates TH1-type immune responses. *Clin Immunol Immunopathol* 1997; **83**: 117-126
- Japanese Gastric Cancer Association. Japanese classification of gastric carcinoma—2nd English edition—response assessment of chemotherapy and radiotherapy for gastric carcinoma: clinical criteria. *Gastric Cancer* 2001; **4**: 1-8
- Olaszewski WL, Kubicka U, Tarnowski W, Bielecki K, Ziolkowska A, Wesolowska A. Activation of human peritoneal immune cells in early stages of gastric and colon cancer. *Surgery* 2007; **141**: 212-221
- Mori T, Shimizu M, Iwaguchi T. Immunological characterization and clinical significance of low mobility cells appearing in the peripheral blood mononuclear cells of cancer patients. *Eur J Cancer Clin Oncol* 1988; **24**: 1463-1469

- 26 **Marutsuka T**, Shimada S, Shiomori K, Hayashi N, Yagi Y, Yamane T, Ogawa M. Mechanisms of peritoneal metastasis after operation for non-serosa-invasive gastric carcinoma: an ultrarapid detection system for intraperitoneal free cancer cells and a prophylactic strategy for peritoneal metastasis. *Clin Cancer Res* 2003; **9**: 678-685
- 27 **Jung M**, Jeung HC, Lee SS, Park JY, Hong S, Lee SH, Noh SH, Chung HC, Rha SY. The clinical significance of ascitic fluid CEA in advanced gastric cancer with ascites. *J Cancer Res Clin Oncol* 2010; **136**: 517-526
- 28 **Sallusto F**, Geginat J, Lanzavecchia A. Central memory and effector memory T cell subsets: function, generation, and maintenance. *Annu Rev Immunol* 2004; **22**: 745-763
- 29 **Berger C**, Jensen MC, Lansdorp PM, Gough M, Elliott C, Riddell SR. Adoptive transfer of effector CD8+ T cells derived from central memory cells establishes persistent T cell memory in primates. *J Clin Invest* 2008; **118**: 294-305
- 30 **Ye SW**, Wang Y, Valmori D, Ayyoub M, Han Y, Xu XL, Zhao AL, Qu L, Gnjjatic S, Ritter G, Old LJ, Gu J. Ex-vivo analysis of CD8+ T cells infiltrating colorectal tumors identifies a major effector-memory subset with low perforin content. *J Clin Immunol* 2006; **26**: 447-456
- 31 **Wang HY**, Wang RF. Regulatory T cells and cancer. *Curr Opin Immunol* 2007; **19**: 217-223
- 32 **Nishikawa H**, Kato T, Hirayama M, Orito Y, Sato E, Harada N, Gnjjatic S, Old LJ, Shiku H. Regulatory T cell-resistant CD8+ T cells induced by glucocorticoid-induced tumor necrosis factor receptor signaling. *Cancer Res* 2008; **68**: 5948-5954
- 33 **Curiel TJ**, Coukos G, Zou L, Alvarez X, Cheng P, Mottram P, Evdemon-Hogan M, Conejo-Garcia JR, Zhang L, Burow M, Zhu Y, Wei S, Kryczek I, Daniel B, Gordon A, Myers L, Lackner A, Disis ML, Knutson KL, Chen L, Zou W. Specific recruitment of regulatory T cells in ovarian carcinoma fosters immune privilege and predicts reduced survival. *Nat Med* 2004; **10**: 942-949
- 34 **Wing K**, Onishi Y, Prieto-Martin P, Yamaguchi T, Miyara M, Fehervari Z, Nomura T, Sakaguchi S. CTLA-4 control over Foxp3+ regulatory T cell function. *Science* 2008; **322**: 271-275
- 35 **Onishi Y**, Fehervari Z, Yamaguchi T, Sakaguchi S. Foxp3+ natural regulatory T cells preferentially form aggregates on dendritic cells in vitro and actively inhibit their maturation. *Proc Natl Acad Sci USA* 2008; **105**: 10113-10118
- 36 **Stanzer S**, Dandachi N, Balic M, Resel M, Samonigg H, Bauernhofer T. Resistance to apoptosis and expansion of regulatory T cells in relation to the detection of circulating tumor cells in patients with metastatic epithelial cancer. *J Clin Immunol* 2008; **28**: 107-114
- 37 **Gnjjatic S**, Altorki NK, Tang DN, Tu SM, Kundra V, Ritter G, Old LJ, Logothetis CJ, Sharma P. NY-ESO-1 DNA vaccine induces T-cell responses that are suppressed by regulatory T cells. *Clin Cancer Res* 2009; **15**: 2130-2139

S- Editor Gou SX L- Editor Webster JR E- Editor Zhang DN

Available online at [www.sciencedirect.com](http://www.sciencedirect.com)

ScienceDirect

journal homepage: [www.JournalofSurgicalResearch.com](http://www.JournalofSurgicalResearch.com)

# The detection of gastric cancer cells in intraoperative peritoneal lavage using the reverse transcription–loop-mediated isothermal amplification method

Akira Yoneda, MD, PhD,\* Ken Taniguchi, MD, PhD, Yasuhiro Torashima, MD, PhD, Seiya Susumu, MD, PhD, Kengo Kanetaka, MD, PhD, Tamotsu Kuroki, MD, PhD, and Susumu Eguchi, MD, PhD

Department of Surgery, Nagasaki University Graduate School of Biomedical Sciences, Nagasaki, Japan

## ARTICLE INFO

### Article history:

Received 27 April 2012  
 Received in revised form  
 29 December 2012  
 Accepted 3 January 2013  
 Available online 25 January 2013

### Keywords:

Gastric cancer  
 RT–LAMP  
 Peritoneal lavage

## ABSTRACT

**Introduction:** To detect a small number of malignant cells, we used a highly sensitive detection system that measures the expression levels of cytokeratin (CK) 19 messenger RNA by reverse transcription–loop-mediated isothermal amplification (RT–LAMP).

**Materials and methods:** We evaluated the clinical relevance of our novel diagnostic method with an RT–LAMP assay using CK19 as a target gene for the detection of free cancer cells in peritoneal lavage and assessed the clinical significance of the molecular diagnosis by survival analysis and frequency of recurrence, with a median follow-up period of 39 mo. We observed 52 patients with gastric cancer who underwent gastrectomy, bypass operation, and exploratory laparotomy.

**Results:** Those 52 patients, who were subjected to both RT–LAMP and cytologic examination, were divided into the following three groups: (1) patients positive by cytology and RT–LAMP (CY+/LAMP+) ( $n = 9$ ), (2) patients positive by LAMP and negative by cytology (CY–/LAMP+) ( $n = 12$ ), and (3) patients negative by both cytology and LAMP (CY–/LAMP–) ( $n = 31$ ). All patients with simultaneous peritoneal dissemination and positive cytology were positive on RT–LAMP. The results of RT–LAMP were statistically significant for recurrence by univariate analysis ( $P < 0.005$ ). Cytology-positive cases had a very poor prognosis, and RT–LAMP-positive cases had a worse prognosis than RT–LAMP-negative cases.

**Conclusions:** Our findings suggest that CK19 RT–LAMP would be useful as an intraoperative diagnostic modality to detect patients with a high risk of recurrence even after clinically curative surgery, who thus require proper adjuvant therapy.

© 2014 Published by Elsevier Inc.

## 1. Introduction

Peritoneal carcinomatosis is the most frequent pattern of recurrence in patients with gastric cancer [1,2]. The prognosis of patients with advanced gastric cancer invading the gastric serosa is very poor even after curative resection, mainly

because of the high incidence of peritoneal recurrence [3]. Recurrence with this pattern is most likely caused by the presence of free cancer cells in the abdominal cavity exfoliated from the serosal surfaces of the primary gastric tumor [4]. Therefore, detection of such micrometastatic cells in the peritoneal cavity is likely to be a useful tool in the selection of

\* Corresponding author. Department of Surgery, Nagasaki University Graduate School of Biomedical Sciences, 1-7-1 Sakamoto, Nagasaki 852-8501, Japan. Tel.: +81 95 819 7316; fax: +81 95 819 7319.

E-mail address: [d06034e@cc.nagasaki-u.ac.jp](mailto:d06034e@cc.nagasaki-u.ac.jp) (A. Yoneda).  
 0022-4804/\$ – see front matter © 2014 Published by Elsevier Inc.  
<http://dx.doi.org/10.1016/j.jss.2013.01.001>

intra or postoperative chemotherapy and for predicting the outcome of such therapy in these cases [5]. In this regard, cytologic examination of lavage fluid obtained at the time of surgery is a conventional method for detecting free cancer cells in peritoneal space. However, the sensitivity of this assay has been reported to be relatively low, ranging from 19% to 30% in gastric cancer invading the serosa [6–9]. As a result, some patients with negative cytology have nevertheless developed peritoneal recurrence. Therefore, there is an urgent need for more sensitive methods to detect micrometastasis in the peritoneal cavity. To detect small numbers of malignant cells among the cytologically negative cases, we developed a highly sensitive detection system that measures the expression levels of cytokeratin (CK) 19 messenger RNA (mRNA) by reverse transcription–loop-mediated isothermal amplification (RT–LAMP). The RT–LAMP method is a new method of gene amplification, the efficacy of which has been reported [10,11]. The reaction is accelerated by the use of two additional loop primers (called loops F and B) [11]. The LAMP method can be conducted simultaneously with reverse transcription from mRNA (RT–LAMP) [10–14]. There are several practical advantages to the RT–LAMP technique: it requires only simple reaction procedures, the compact and inexpensive incubator or turbidimeter equipment costs <\$5000, and <1 h is needed to obtain the final results [11–15]. Application of the LAMP technique has been reported for breast and lung cancers [16–18]. This technique might be one of the most promising candidates for analyzing the genetic features of samples obtained during surgery.

CK proteins of the intermediate filaments of epithelial cells have been used as specific markers for tumor cells of epithelial origin [19,20]. In the present study, we evaluated the clinical relevance of a new diagnostic method using an RT–LAMP assay with CK19 as the target gene for the detection of free cancer cells in the peritoneal lavage and assessed the clinical significance of the molecular diagnosis by survival analysis and frequency of recurrence.

## 2. Materials and methods

### 2.1. Cell lines

A sensitivity assay for detecting a gastric cancer cell line was performed. The human gastric cancer cell line MKN-45, obtained from the Riken Cell Bank (Institute of Physical and Chemical Research, Saitama, Japan), was incubated in RPMI-1640 medium containing 10% fetal calf serum (Invitrogen, Carlsbad, CA) at 37°C in 5% CO<sub>2</sub>.

### 2.2. Patients

Between May 2007 and November 2008, we observed 52 patients (35 males and 17 females; mean age, 67.5 ± 2.8 y) with gastric cancer who underwent gastrectomy (*n* = 45), bypass operation (*n* = 2), and exploratory laparotomy (*n* = 7) for histologically proven gastric cancer at the Department of Surgery, Nagasaki University. Written informed consent for participation in this study was obtained from all the patients. All were followed up for a median of 39 mo (range,

6–51 mo) or until death. The primary tumor was resected in 45 of the 52 patients (five patients had peritoneal dissemination but underwent resection of their primary tumor because of the stenosis and bleeding caused by primary tumor as a palliative treatment) but was unresectable in seven patients because of peritoneal dissemination and positive cytology. These seven patients underwent a bypass operation or exploratory laparotomy. The resected specimens were histologically examined by hematoxylin and eosin staining according to the general rules of the Japanese Classification of Gastric Carcinoma [21]. Clinicopathologic features of the patients are shown in Table 1.

### 2.3. RT–LAMP reaction

LAMP primers targeting the CK19 complementary DNA were designed based on a past report [22] (Fig. 1). To quantify and prove the integrity of isolated RNA, we also performed RT–LAMP for β-actin.

The RT–LAMP method was carried out on 25 μL of the total reaction mixture with a Loopamp RNA amplification kit (Eiken Chemical Co, Tokyo, Japan) containing 40 pmol each of the forward and backward inner primers, 5 pmol each of the outer primers F3 and B3, 20 pmol each of the loop primers loops F and B, 35 pmol of dNTPs, 20 μL of Betamine, 0.5 μM Tris–HCL (pH 8.8), 0.25 μM KCL, 0.25 μM (NH<sub>4</sub>)SO<sub>4</sub>, 0.2 μM MgSO<sub>4</sub>, 0.2% Tween 20, 1.0 μL of Enzyme Mix (Bst DNA polymerase and

**Table 1 – Clinicopathologic factors were determined according to the Japanese classification of gastric carcinoma.**

|   | Number of patients |
|---|--------------------|
| Total cases   | 52                 |
| Age (y)   | 67.5 ± 2.8         |
| Sex: male/female  | 35/17              |
| Depth of tumor invasion   |                    |
| M   | 11                 |
| SM  | 13                 |
| MP  | 6                  |
| SS  | 9                  |
| SE and SI   | 13                 |
| Lymph node metastasis   |                    |
| N0  | 22                 |
| N1  | 13                 |
| N2  | 13                 |
| N3  | 4                  |
| Peritoneal metastasis   |                    |
| Absent  | 40                 |
| Present   | 12                 |
| Cytology  |                    |
| Negative  | 43                 |
| Positive  | 9                  |
| Stages  |                    |
| IA  | 18                 |
| IB  | 7                  |
| II  | 8                  |
| III   | 4                  |
| IV  | 15                 |
| M = mucosa; SM = submucosa; MP = muscularis propria; SS = subserosa; SE = serosa exposed; SI = serosa infiltrating. |                    |

F3 :  
 CCTCCTACCTGGCAAGGT  
 B3 : ATGCGCAGAGCCTGTC  
 FIP (F1c+F2):TAGTGGCTGTAGTCGCGG  
 GAAACGGCGAGCTAGAGGAGAA  
 BIP (B1c+B2):CGGGACAAGATTCTTGGTGCCAAAGT  
 CATCTGCAGCCAGACG  
 loopF : AGGCCCTGCTTCTGGTAC  
 loopB : CCTGCAGATCGACAATGCC

**Fig. 1 – Primer design for the detection of CK19 mRNA by RT–LAMP.**

avian myeloblastosis virus reverse transcriptase), and 5 µL of RNA at a constant temperature of 63.5°C for 60 min. Temperature control for the LAMP reaction and turbidity measurement was achieved using a turbidimeter (LA-200; Teramecs Co, Kyoto, Japan) especially developed for DNA analysis by LAMP reaction.

**2.4. Sensitivity evaluation of RT–LAMP on CK19 mRNA detection**

A fundamental experiment was performed to determine the sensitivity of the RT–LAMP method for detecting gastric cancer cells in peripheral blood mononuclear cells (PBMCs). Peripheral venous blood was obtained from healthy volunteers. Gastric cancer MKN-45 cells were serially diluted from  $1 \times 10^6$  cells to one cell per  $1 \times 10^7$  PBMCs. The mRNA was extracted from each cell fraction, and RT–LAMP for CK19 mRNA was performed.

**2.5. Preparation of peritoneal floating cells**

At the beginning of the operation, before the manipulation of the tumor, 400 mL of physiological saline was introduced into the upper abdominal cavity and recovered after being gently stirred. Part of the peritoneal lavage fluid was subjected to conventional cytology after standard Papanicolaou staining, and the remaining fluid was immediately centrifuged at 2000 rpm for 10 min. The pellets of lavaged fluid were rinsed

with phosphate-buffered saline, dissolved in RNAlater solution (Ambion, Austin, TX), and stored at –80°C until use.

**2.6. mRNA extraction**

The mRNA was extracted using the Dynabeads mRNA DIRECT kit (Veritas, Tokyo, Japan) according to the manufacturer’s instructions. Briefly, collected cells were lysed by the lysis or binding buffer, and the released mRNA and its poly (A) residue were hybridized with oligo (dT) conjugated with Dynabeads; then, this complex was immobilized onto the surface of magnetic beads. Contaminating components were washed away by repeated steps of separation and resuspension in washing buffer. Finally, the purified mRNA was eluted from the particles.

**2.7. RT–LAMP on mRNA derived from peritoneal lavage**

Twenty-five microliters of reaction mixture was applied to each reaction. Positive control primers (β-actin) and a negative control mixture (PBMC-derived sample) were used for all reactions.

**2.8. Statistical analysis**

All statistical analyses were performed using StatView 5.0 software (SAS Institute, Cary, NC). The chi-square test was used to evaluate the correlation between positive results and clinicopathologic factors, and the univariate analysis was used to evaluate the results of RT–LAMP and recurrence. Survival curves were calculated using the Kaplan–Meier method. The survival curves were compared using the log-rank test.  $P < 0.05$  was considered statistically significant.

**3. Results**

**3.1. Evaluation of the sensitivity of RT–LAMP for identifying gastric carcinoma cell line**

As few as  $10^0$  MKN-45 cells in  $10^7$  normal PBMCs were detectable with the RT–LAMP procedures targeting CK19–mRNA using extracted mRNA of cell mixtures lysate (Fig. 2).

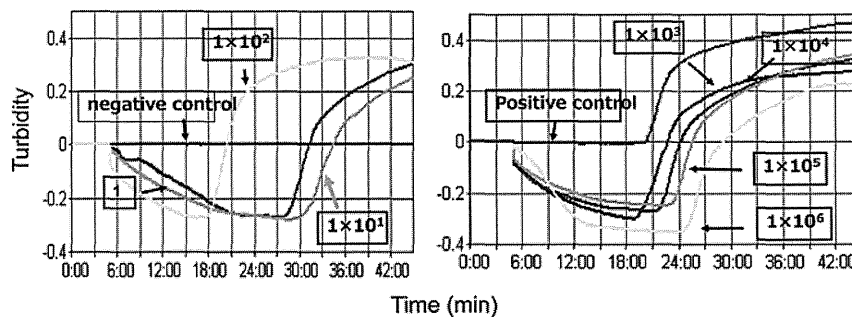


**Fig. 2 – Sensitivity analysis of the RT–LAMP method. As few as  $10^0$  MKN-45 cells in  $10^7$  normal PBMCs were detectable with the RT–LAMP procedures targeting CK19 mRNA using extracted mRNA of the cell mixture lysate.**

### 3.2. Detection of cancer cells in intraoperative peritoneal lavage

The mRNA of  $\beta$ -actin, a housekeeping gene, was detected in all the present samples. RT–LAMP reaction diagnosis significantly correlated with lymph node metastasis, depth of invasion, lymphatic invasion, and vessel invasion (Table 2). The total of 52 patients who were subjected to both RT–LAMP and cytologic examination were divided into the following three groups: (1) patients positive by cytology and RT–LAMP (CY+/LAMP+) ( $n = 9$ ), (2) patients positive by LAMP and negative by cytology (CY–/LAMP+) ( $n = 12$ ), and (3) patients negative by both cytology and LAMP (CY–/LAMP–) ( $n = 31$ ). The stage of each groups was showed on Table 2. There were no patients negative by LAMP and positive by cytology; all patients with simultaneous peritoneal dissemination and positive cytology were positive on RT–LAMP. Simultaneous peritoneal dissemination at surgery or staging laparoscopy was detected in 12 patients (nine in the group CY+/LAMP+ and three in the group CY–/LAMP+). No patients with negative RT–LAMP and negative CY status had recurrence after surgery. The results of RT–LAMP were statistically significant for recurrence by univariate analysis ( $P < 0.005$ ). Figure 3 shows the overall survival (Fig. 3A), recurrence-free survival (Fig. 3B), and peritoneal recurrence-free survival

(Fig. 3C) curves for the three patient groups subjected to both RT–LAMP and cytologic examination. Figure 3 shows that cytology-positive cases had a very poor prognosis and that cases with negative cytology but positive RT–LAMP had a worse prognosis than that of the cases who were RT–LAMP negative.

## 4. Discussion

Although the standard surgical lymphadenectomy for gastric cancer has been established and applied, patients with advanced stages of this cancer continue to face a poor prognosis. A previous study suggested that the presence of free cancer cells in peritoneal lavage was responsible for the formation of micrometastasis and subsequent extensive dissemination [23,24]. Cytologic examination aimed at the detection of these cells, therefore, has been generally accepted as the golden criterion for the prediction of peritoneal recurrence, and this procedure has been incorporated in the Japanese staging system for gastric cancer [21]. However, peritoneal recurrence sometimes occurs in patients with negative cytology, which indicates the lack of sensitivity of conventional cytologic examination for the prediction of peritoneal recurrence. We believe that it is difficult to confirm peritoneal metastasis from cytology because of its low sensitivity. Jung *et al.* [25] reported that even in patients with clinically diagnosed carcinomatosis with ascites, only 54% of patients were positive for cytology.

Thus, a more sensitive assay for the detection of peritoneal micrometastasis is required. New, simple, and rapid molecular techniques for the detection of target genes have been developed in recent years, and one of these is the LAMP reaction. This reaction is a novel approach to the DNA amplification of target sequences, providing high sensitivity, specificity, and rapidity under isothermal conditions. The LAMP reaction relies on autocycling strand displacement DNA synthesis that is performed with a DNA polymerase with high-strand displacement activity and four specific primers recognizing six independent sequences. Specifically, it synthesizes a large amount of amplification products, comprising a mixture of stem–loop DNA and cauliflower-like structures with multiple loops (except for the loops that are hybridized by the inner primer) and prime strand displacement DNA. When the target DNA is amplified by LAMP reaction, a white precipitate derived from magnesium pyrophosphate (a byproduct of LAMP reaction) is observed [10]; thus, the LAMP method does not require special reagents or electrophoresis to detect the amplified DNA. Amplification of the targeted gene is detectable in real-time fashion by an increase of the turbidity of the solution.

CK19 has been shown to be widely expressed by cancer cells of epithelial origin but not by lymphoid or hematopoietic cells [26]. Among some 20 different isotypes, CK19 and CK20 are expressed more selectively by mucosal epithelial cells than are the others [27]. It has been reported that CK19 is superior to CK20 in detecting circulating cancer cells using reverse transcription–polymerase chain reaction (RT–PCR) in peripheral blood from patients with gastric cancer [28]. Thus, this molecule may be a suitable general marker of

**Table 2 – Correlation between RT–LAMP diagnosis of peritoneal lavage and clinicopathologic parameters and the stage of each groups.**

|                         | Expression of CK19 mRNA (RT–LAMP) |          | P-value |
|-------------------------|-----------------------------------|----------|---------|
|                         | Positive                          | Negative |         |
| Number of patients      | 21                                | 31       |         |
| Sex                     |                                   |          |         |
| Male                    | 14                                | 21       | NS      |
| Female                  | 7                                 | 10       |         |
| Age (y)                 | 62.45                             | 67.8     | NS      |
| Depth of tumor invasion |                                   |          |         |
| M                       | 0                                 | 11       |         |
| SM                      | 0                                 | 13       |         |
| MP                      | 3                                 | 3        | 0.00001 |
| SS                      | 6                                 | 3        |         |
| SE and SI               | 12                                | 1        |         |
| Lymph node metastasis   |                                   |          |         |
| –                       | 3                                 | 23       | 0.00002 |
| +                       | 18                                | 8        |         |
| Lymphatic invasion      |                                   |          |         |
| –                       | 1                                 | 16       | 0.0091  |
| +                       | 11                                | 15       |         |
| Vessel invasion         |                                   |          |         |
| –                       | 1                                 | 18       | 0.0033  |
| +                       | 11                                | 13       |         |

M = mucosa; SM = submucosa; MP = muscularis propria; SS = subserosa; SE = serosa exposed; SI = serosa infiltrating.

CY+/LAMP+ ( $n = 9$ ): stage IV,  $n = 9$ .

CY–/LAMP+ ( $n = 12$ ): stage II,  $n = 4$ ; stage III,  $n = 3$ ; and stage IV,  $n = 5$ .

CY–/LAMP– ( $n = 31$ ): stage IA,  $n = 19$ ; stage IB,  $n = 6$ ; stage II,  $n = 4$ ; and stage III,  $n = 2$ .

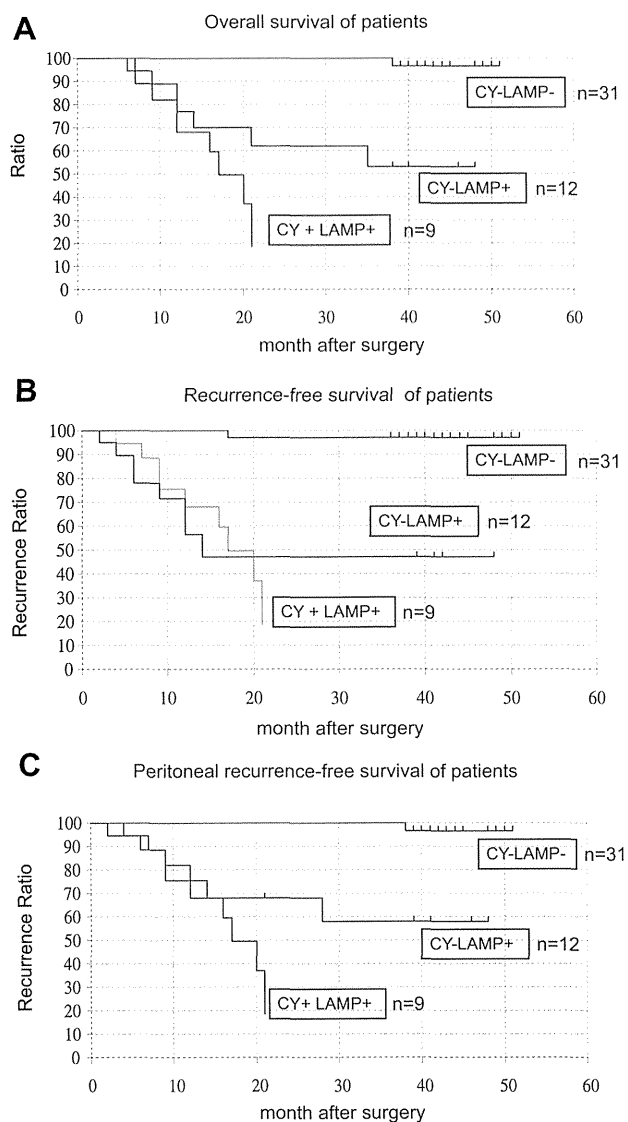


**Fig. 3 – (A) Overall survival curves of patients stratified according to the results of cytology and RT–LAMP. Significant differences between the CY–LAMP– and CY–LAMP+ groups were found ( $P < 0.05$ ). (B) Recurrence-free survival curves of patients stratified according to the results of cytology and RT–LAMP. Significant differences between the CY–LAMP– and CY–LAMP+ groups were found ( $P < 0.05$ ). (C) Peritoneal recurrence-free survival curves of patients stratified according to the results of cytology and RT–LAMP. Significant differences between the CY–LAMP– and CY–LAMP+ groups were found ( $P < 0.05$ ).**

micrometastasis in peritoneal lavage of patients with gastric cancer. LAMP primers were generated to detect the CK19 sequence, and the performance of the RT–LAMP reaction to detect gastric cancer cells was tested. Only cells of epithelial origin were detected by this technique, with sensitivity to concentrations as low as one cell per  $10^7$  normal PBMCs. CK expression was observed in the RT–LAMP reaction, presumably because of its high specificity, which requires the

recognition of six independent sequences within the target molecule [22].

The development of a rapid technique for detecting cancer cells in peritoneal lavage of patients with gastric cancer using the RT–LAMP reaction is herein described. Among the patients with negative cytology, those with a positive RT–LAMP reaction had a poorer prognosis than those with negative RT–LAMP reaction results. In three patients, laparotomy was performed preceding the staging laparoscopy to verify negative cytology and the lack of obvious peritoneal dissemination. However, peritoneal dissemination was found after open exploration, and further surgery was canceled. For all these patients, the results of the RT–LAMP reaction were positive. As these results indicated, even when cancer cells are not found by cytology, the RT–LAMP method could be used to determine the necessity of surgery. Our results demonstrated significant correlations between the CK19 findings and depth of cancer invasion, the presence and extent of lymph node metastasis, and the vessel and lymphatic invasion. In this sense, CK19 expressed by free cancer cells in peritoneal lavage could be a candidate molecular marker indicating high invasive potential and aggressive behavior in gastric cancers. It is remarkable that the results of the RT–LAMP method correlated not only with the peritoneal recurrences but also with other fashions without tumor exposure to the serosa. Minor diffusion of tumor cells might occur during the migration through the lymphatic vessels [29–31], and further evaluation would be needed around the origin.

The benefit of adjuvant chemotherapies in solid tumors is known to be related to the amount of remnant tumor burden. Therefore, patients with positive RT–LAMP without macroscopic peritoneal dissemination seem good candidates for a cure through appropriate adjuvant therapy. Kodera et al. [32] reported that postoperative S-1 monotherapy could make no difference in survival between patients with visible peritoneal deposits and patients with only positive cytology. To improve the prognosis, it is crucial to identify high-risk patients at a much earlier phase of peritoneal dissemination. As molecular approaches such as RT–LAMP and RT–PCR analysis have the potential to do just that, adjuvant therapy could eliminate remnant cancer cells detected only by molecular diagnosis. Limitations include a small sample size.

The RT–LAMP technique could be performed as an alternative to an intraoperative cytologic examination. Because of its high sensitivity and rapidity, this method could provide an opportunity to perform a reliable tailor-made surgery for gastric cancers as a common procedure in general hospitals. However, the present study has some limitations. First, this study included a too small sample size to assess whether RT–LAMP positivity could be independent prognostic biomarker in cytology-negative patients. Second, this molecular-based method is known to be concerned with a high false-positive rate. Kodera et al. [33] reported that when the cutoff value was set at 0.1 for CEA mRNA, the false-positive rate of CEA RT–PCR exceeded 10%. To confirm the efficacy of the RT–LAMP method, additional efforts are necessary to assess the outcome of the treatment of patients with RT–LAMP-positive peritoneal lavage findings in larger sample size.

## 5. Conclusion

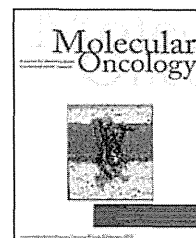
Our findings suggest that CK19 RT–LAMP would be useful as an intraoperative diagnostic modality to detect potential high-risk patients who may develop recurrence even after clinically curative surgery and guide choices about proper adjuvant therapy.

## REFERENCES

- [1] Yoo CH, Noh SH, Shin DW, et al. Recurrence following curative resection for gastric carcinoma. *Br J Surg* 2000;87:236.
- [2] Maehara Y, Hasuda S, Koga T, et al. Postoperative outcome and sites of recurrence in patients following curative resection of gastric cancer. *Br J Surg* 2000;87:353.
- [3] Baba H, Korenaga D, Okamura T, et al. Prognostic factors in gastric cancer with serosal invasion. Univariate and multivariate analyses. *Arch Surg* 1989;124:1061.
- [4] Koga S, Kaibara N, Iitsuka Y, et al. Prognostic significance of intraperitoneal free cancer cells in gastric cancer patients. *J Cancer Res Clin Oncol* 1984;108:236.
- [5] Bonenkamp JJ, Songun I, Hermans J, et al. Prognostic value of positive cytology findings from abdominal washings in patients with gastric cancer. *Br J Surg* 1996;83:672.
- [6] Ikeguchi M, Oka A, Tsujitani S, et al. Relationship between area of serosal invasion and intraperitoneal free cancer cells in patients with gastric cancer. *Anticancer Res* 1994;14:2131.
- [7] Burke EC, Karpeh MS Jr, Conlon KC, et al. Peritoneal lavage cytology in gastric cancer: an independent predictor of outcome. *Ann Surg Oncol* 1998;5:411.
- [8] Kodera Y, Yamamura Y, Shimizu Y, et al. Peritoneal washing cytology: prognostic value of positive findings in patients with gastric carcinoma undergoing a potentially curative resection. *J Surg Oncol* 1999;72:60. discussion 64–65.
- [9] Suzuki T, Ochiai T, Hayashi H, et al. Importance of positive peritoneal lavage cytology findings in the stage grouping of gastric cancer. *Surg Today* 1999;29:111.
- [10] Notomi T, Okayama H, Masubuchi H, et al. Loop-mediated isothermal amplification of DNA. *Nucleic Acids Res* 2000;28:E63.
- [11] Nagamine K, Hase T, Notomi T. Accelerated reaction by loop-mediated isothermal amplification using loop primers. *Mol Cell Probes* 2002;16:223.
- [12] Hirayama H, Kageyama S, Moriyasu S, et al. Rapid sexing of bovine preimplantation embryos using loop-mediated isothermal amplification. *Theriogenology* 2004;62:887.
- [13] Parida M, Posadas G, Inoue S, et al. Real-time reverse transcription loop-mediated isothermal amplification for rapid detection of West Nile virus. *J Clin Microbiol* 2004;42:257.
- [14] Ushio M, Yui I, Yoshida N, et al. Detection of respiratory syncytial virus genome by subgroups-A, B specific reverse transcription loop-mediated isothermal amplification (RT-LAMP). *J Med Virol* 2005;77:121.
- [15] Mori Y, Nagamine K, Tomita N, et al. Detection of loop-mediated isothermal amplification reaction by turbidity derived from magnesium pyrophosphate formation. *Biochem Biophys Res Commun* 2001;289:150.
- [16] Tsujimoto M, Nakabayashi K, Yoshidome K, et al. One-step nucleic acid amplification for intraoperative detection of lymph node metastasis in breast cancer patients. *Clin Cancer Res* 2007;13:4807.
- [17] Maeda J, Inoue M, Nakabayashi K, et al. Rapid diagnosis of lymph node metastasis in lung cancer with loop-mediated isothermal amplification assay using carcinoembryonic antigen-mRNA. *Lung Cancer* 2009;65:324.
- [18] Tamaki Y, Akiyama F, Iwase T, et al. Molecular detection of lymph node metastases in breast cancer patients: results of a multicenter trial using the one-step nucleic acid amplification assay. *Clin Cancer Res* 2009;15:2879.
- [19] Moll R, Franke WW, Schiller DL, et al. The catalog of human cytokeratins: patterns of expression in normal epithelia, tumors and cultured cells. *Cell* 1982;31:11.
- [20] Osborn M, van Lessen G, Weber K, et al. Differential diagnosis of gastrointestinal carcinomas by using monoclonal antibodies specific for individual keratin polypeptides. *Lab Invest* 1986;55:497.
- [21] Japanese classification of gastric carcinoma: 3rd English edition. *Gastric Cancer* 14:101.
- [22] Horibe D, Ochiai T, Shimada H, et al. Rapid detection of metastasis of gastric cancer using reverse transcription loop-mediated isothermal amplification. *Int J Cancer* 2007;120:1063.
- [23] Wong SC, Yu H, So JB. Detection of telomerase activity in gastric lavage fluid: a novel method to detect gastric cancer. *J Surg Res* 2006;131:252.
- [24] Ishigami S, Sakamoto A, Uenosono Y, et al. Carcinoembryonic antigen messenger RNA expression in blood can predict relapse in gastric cancer. *J Surg Res* 2008;148:205.
- [25] Jung M, Jeung HC, Lee SS, et al. The clinical significance of ascitic fluid CEA in advanced gastric cancer with ascites. *J Cancer Res Clin Oncol* 136:517.
- [26] Ruud P, Fodstad O, Hovig E. Identification of a novel cytokeratin 19 pseudogene that may interfere with reverse transcriptase-polymerase chain reaction assays used to detect micrometastatic tumor cells. *Int J Cancer* 1999;80:119.
- [27] Moll R, Lowe A, Laufer J, et al. Cytokeratin 20 in human carcinomas. A new histodiagnostic marker detected by monoclonal antibodies. *Am J Pathol* 1992;140:427.
- [28] Majima T, Ichikura T, Takayama E, et al. Detecting circulating cancer cells using reverse transcriptase-polymerase chain reaction for cytokeratin mRNA in peripheral blood from patients with gastric cancer. *Jpn J Clin Oncol* 2000;30:499.
- [29] Yamagata K, Kumagai K. Experimental study of lymphogenous peritoneal cancer dissemination: migration of fluorescent-labelled tumor cells in a rat model of mesenteric lymph vessel obstruction. *J Exp Clin Cancer Res* 2000;19:211.
- [30] Sleeman JP, Thiele W. Tumor metastasis and the lymphatic vasculature. *Int J Cancer* 2009;125:2747.
- [31] Hirakawa S. From tumor lymphangiogenesis to lymphovascular niche. *Cancer Sci* 2009;100:983.
- [32] Kodera Y, Ito S, Mochizuki Y, et al. A phase II study of radical surgery followed by postoperative chemotherapy with S-1 for gastric carcinoma with free cancer cells in the peritoneal cavity (CCOG0301 study). *Eur J Surg Oncol* 2009;35:1158.
- [33] Kodera Y, Nakanishi H, Ito S, et al. Prognostic significance of intraperitoneal cancer cells in gastric carcinoma: analysis of real time reverse transcriptase-polymerase chain reaction after 5 years of followup. *J Am Coll Surg* 2006;202:231.

available at [www.sciencedirect.com](http://www.sciencedirect.com)

ScienceDirect

[www.elsevier.com/locate/molonc](http://www.elsevier.com/locate/molonc)

## Enhanced expression of retinoic acid receptor alpha (*RARA*) induces epithelial-to-mesenchymal transition and disruption of mammary acinar structures

Ayano Doi<sup>a</sup>, Kosuke Ishikawa<sup>a,b</sup>, Nao Shibata<sup>a</sup>, Emi Ito<sup>c</sup>, Jiro Fujimoto<sup>a,b</sup>, Mizuki Yamamoto<sup>a</sup>, Hatsuki Shiga<sup>b</sup>, Hiromi Mochizuki<sup>b</sup>, Yoshifumi Kawamura<sup>b</sup>, Naoki Goshima<sup>d</sup>, Kentaro Semba<sup>a,e,\*</sup>, Shinya Watanabe<sup>c</sup>

<sup>a</sup>Department of Life Science and Medical Bioscience, School of Advanced Science and Engineering, Waseda University, 2-2 Wakamatsu-cho, Shinjuku-ku, Tokyo 162-8480, Japan

<sup>b</sup>Japan Biological Informatics Consortium (JBIC), 2-45 Aomi, Koto-ku, Tokyo 135-8073, Japan

<sup>c</sup>Division of Gene Expression Analysis, Translational Research Center (Tokyo Branch), Fukushima Medical University, Shibuya-ku, Tokyo 151-0051, Japan

<sup>d</sup>Quantitative Proteomics Team, Molecular Profiling Research Center for Drug Discovery (molprof), National Institute of Advanced Industrial Science and Technology (AIST), 2-4-7 Aomi, Koto-ku, Tokyo 135-0064, Japan

<sup>e</sup>Division of Gene Function Analysis, Translational Research Center, Fukushima Medical University, 1 Hikarigaoka, Fukushima-city, Fukushima 960-1295, Japan

## ARTICLE INFO

## Article history:

Received 29 May 2014

Received in revised form

15 September 2014

Accepted 15 September 2014

Available online 22 September 2014

## Keywords:

3D culture

Gene amplification

Breast cancer

EMT

ERBB2

RARA

## ABSTRACT

The early steps of mammary tumorigenesis include loss of epithelial cell polarity, escape from anoikis, and acquisition of proliferative capacity. The genes responsible for these processes are predicted to be early diagnostic markers or new therapeutic targets. Here we tested 51 genes coamplified with ERBB2 in the 17q12–21 amplicon for these tumorigenic activities using an MCF10A 3D culture-based screening system. We found that overexpression of retinoic acid receptor  $\alpha$  (*RARA*) disrupted normal acinar structure and induced epithelial-to-mesenchymal transition (EMT). The mRNA levels of known EMT-inducing factors, including SLUG, FOXC2, ZEB1, and ZEB2, were significantly increased upon *RARA* overexpression. Knockdown of ZEB1 suppressed the *RARA*-mediated EMT phenotype. These results suggest that overexpression of *RARA* enhances malignant transformation during mammary tumorigenesis.

© 2014 Federation of European Biochemical Societies. Published by Elsevier B.V. All rights reserved.

**Abbreviations:** Dox, doxycycline; RAR $\alpha$ , retinoic acid receptor alpha; ERBB2, v-erbB-2 avian erythroblastic leukemia viral oncogene homolog B2; ZEB, zinc finger E-box-binding homeobox; FOXC2, forkhead box protein C2; RXR, retinoid X receptor; TGF $\beta$ , transforming growth factor beta; EMT, epithelial-to-mesenchymal transition; DCIS, ductal carcinoma in situ; IBC, invasive breast cancer; MOI, multiplicity of infection; TRE, tetracycline responsive element; LBD, ligand-binding domain; RARE, retinoic acid response element; ER, estrogen receptor; ATRA, all-trans retinoic acid; BCSC, breast cancer stem cell; MaSC, mammary stem cell.

\* Corresponding author. Department of Life Science and Medical Bioscience, School of Advanced Science and Engineering, Waseda University, 2-2 Wakamatsu-cho, Shinjuku-ku, Tokyo 162-8480, Japan. Tel.: +81 3 5369 7320.

E-mail addresses: [ad0i\\_ioda@yahoo.co.jp](mailto:ad0i_ioda@yahoo.co.jp) (A. Doi), [IshikawaKosuke@gmail.com](mailto:IshikawaKosuke@gmail.com) (K. Ishikawa), [ksemba@waseda.jp](mailto:ksemba@waseda.jp) (K. Semba).

<http://dx.doi.org/10.1016/j.molonc.2014.09.005>

1574-7891/© 2014 Federation of European Biochemical Societies. Published by Elsevier B.V. All rights reserved.

## 1. Introduction

The majority of breast cancers originate from the epithelial cell layers and progress through a continuum of changes to malignancy. Ductal carcinoma *in situ* (DCIS) is an early premalignant stage of breast cancer progression and is recognized as the proliferation of neoplastic epithelial cells within the duct, surrounded by myoepithelial cells and an intact basement membrane. DCIS is the most common type of non-invasive breast cancer in women, yet has the potential to progress towards malignant invasive breast cancer (IBC) and subsequently metastatic cancer (Espina and Liotta, 2011).

Three-dimensional (3D) culture of mammary epithelial cells embedded in Matrigel is an *in vitro* culture system for understanding the biological processes and signaling pathways that lead to the disruption of epithelial architecture at the early stages of mammary tumorigenesis *in vivo* (Debnath and Brugge, 2005; Vargo-Gogola and Rosen, 2007; Yamada and Cukierman, 2007). Matrigel is rich in basement membrane proteins, such as type IV collagen, laminin, and heparan sulfate proteoglycan (Kleinman et al., 1982). When cultured in Matrigel, MCF10A, a spontaneously immortalized but non-transformed human breast epithelial cell line, forms 3D acinar structures characterized by hollow lumens surrounded by polarized and growth-arrested luminal epithelial cells. These structures arise through changes in many biological processes including proliferation, cell polarity, apoptosis, and cell cycle distribution, and resemble mammary acini *in vivo*, which constitute the multiple lobular units at the end of the mammary ducts (Vargo-Gogola and Rosen, 2007; Debnath et al., 2003).

The amplification and overexpression of *ERBB2* in breast cancer is correlated with poor prognosis due to an increased rate of metastasis and chemotherapy resistance. In general, this gene is overexpressed in 50–60% of DCIS (Lu et al., 2009). Muthuswamy et al. (2001) showed that activation of *ERBB2* in 3D-cultured MCF10A cells resulted in aberrant multi-acinar structures with filled lumens, similar to *ERBB2*-overexpressing DCIS *in vivo*. These cells, however, lacked an invasive phenotype, inconsistent with high metastatic rates of clinical *ERBB2*-positive breast cancer, suggesting the existence of other cofactors necessary for malignant progression. Previous studies have shown coexpression of genes such as *TGFB*, *RHOG*, and *FOS* with *ERBB2* induced invasive behaviors in the MCF10A 3D culture system (Seton-Rogers et al., 2004; Witt et al., 2006). However, the clinical significance of these observations remains to be evaluated.

*ERBB2* gene is not amplified alone, but is coamplified together with adjacent genes on the same chromosomal segment (Bieche et al., 1996; Kauraniemi et al., 2001). Given that breast tumors with gene amplification on the distal side of the chromosome 17q12–21 containing *KRT20* and *KRT19* are more aggressive than tumors with amplification restricted to the small region adjacent to *ERBB2* (Lamy et al., 2011; Jacot et al., 2013), it is likely that the other genes localized in the same amplicon as *ERBB2* play a significant role in breast cancer progression.

Here, we established an MCF10A 3D culture-based screening system to identify genes that disrupt acini

formation with or without oncogenic *ERBB2* (*ERBB2VE*) expression. We found that overexpression of retinoic acid receptor alpha gene (*RARA*) in the 17q12–21 amplicon induces both the collapse of luminal morphology and an invasive phenotype. We also found that *RARA* upregulated EMT-inducing transcription factors such as *SLUG*, *FOXC2*, *ZEB1*, and *ZEB2*, and TGF- $\beta$ –SMAD signaling-activating factors including *TGFBR1*, *TGFBR2*, *TGFB2*, and *SMAD3*. Of these genes, *ZEB1* in particular was identified as an essential gene in *RARA*-induced EMT.

Our studies propose a model in which overexpression of *RARA* resulting from gene amplification contributes to the progression of mammary epithelial cell transformation towards more malignant invasive phenotypes through stimulation of the EMT interactome.

## 2. Materials and methods

### 2.1. Cell culture

MCF10A cells were purchased from the American Type Culture Collection (ATCC). Cells were maintained in growth medium consisting of DMEM/F12 (Invitrogen) supplemented with 5% horse serum (Invitrogen), 20 ng/mL human epidermal growth factor (EGF) (BD), 0.5  $\mu$ g/mL hydrocortisone (Sigma), 100 ng/mL cholera toxin (List Biological Laboratories), 10  $\mu$ g/mL insulin (Sigma), 100  $\mu$ g/mL streptomycin (Meiji-Seika), and 100 U/mL penicillin (Meiji-Seika).

### 2.2. Generation of MCF10A cell clones

A DNA fragment of rtTA-Advanced (Clontech) was ligated into an EF1 $\alpha$  promoter-driven plasmid followed by the insertion of IRES-neo. MCF10A cells were transfected with the resultant plasmid pEF-rtTA-Advanced-IRES-neo by calcium phosphate transfection and selected with 800  $\mu$ g/mL G418 (MCF10A/Tet-on). For generating clones inducibly-expressing *ERBB2*<sup>V659E</sup>, the MCF10A/Tet-on clones were cotransfected with two vectors, a puromycin-resistant gene expression vector and a Tet-responsive (Clontech) *ERBB2VE* expression vector (pTRE-Tight-*ERBB2VE*) (1:25 ratio), and selected with 0.5  $\mu$ g/mL puromycin (MCF10A/Tet-on/TRE-*ERBB2VE*). The MCF10A/Tet-on and MCF10A/Tet-on/TRE-*ERBB2VE* clones were then transfected with a vector encoding a murine ecotropic retroviral receptor (pLenti6/Ubc/mSlc7a1, Addgene) and selected with 15  $\mu$ g/mL blasticidin (MCF10A/Tet-on/Eco and MCF10A/Tet-on/TRE-*ERBB2VE*/Eco, respectively). During serial cloning steps, we selected MCF10A clones with the ability to form hollow acini-like structures as most suitable for 3D culture-based screening.

### 2.3. Viral infection

The construction of the pMXs retroviral vectors and retroviral packaging was performed as previously described (Saito et al., 2012). Lentiviral packaging was performed by cotransfection of 293T cells with HIV-based vectors including an expression construct and the pPACK packaging plasmids (System

Biosciences). MCF10A cells were seeded at a density of  $2.0 \times 10^5$  cells in each well of a 12-well plate, followed by infection with a 1:1 mixture of diluted viruses and growth medium the next day. After 24 h for retroviruses, or 16–20 h for lentiviruses, the viral supernatant was replaced with growth medium for an additional 24 h period following which the cells were moved to new dishes.

#### 2.4. Three-dimensional morphogenesis assay

Forty microliters of Matrigel (growth factor reduced, BD) was added to each well of 48-well plates and then the plates were incubated at 37 °C to allow solidification of the Matrigel. MCF10A cells were trypsinized and resuspended in assay medium (DMEM/F12 supplemented with 2% horse serum, 0.5 µg/mL hydrocortisone, 100 ng/mL cholera toxin, 10 µg/mL insulin, 100 µg/mL streptomycin, and 100 U/mL penicillin). Five thousand cells were seeded onto the surface of the solidified Matrigel in a mixture of 400 µL of assay medium containing 5 ng/mL EGF and 2% Matrigel. On day 4, the assay medium supplemented with 5 ng/mL EGF and 2% Matrigel was replaced, and from day 7 the liquid medium was replaced with fresh assay medium containing 1 ng/mL EGF and 2% Matrigel every 4 days. For assays with type I collagen, Matrigel was mixed with a bovine collagen solution (PureCol, Advanced BioMatrix) at a final concentration of 50% Matrigel and 1.2 mg/mL collagen I, and 50 µL of the mixture was used to coat 48-well plates. Before mixing, the collagen I-PureCol was neutralized by addition of  $10 \times$  PBS and 100 mM NaOH (10 $\times$ ), and the pH was adjusted to 7.2–7.6. Cells were seeded on the underlayer using the same procedure described above.

#### 2.5. Antibodies

For immunoblotting, the following antibodies were used.  $\alpha$ -Tubulin (DM1A), Sigma–Aldrich (T9026); FLAG M2, Sigma; Neu (ERBB2), Santa Cruz (sc-284); E-cadherin, BD (610182); N-cadherin, BD (610921); Vimentin (D21H3), Cell Signaling (#5741S); RAR $\alpha$ , Cell Signaling (#2554S); Akt1 (2H10), Cell Signaling (#2967); phospho-Akt (Ser473), Cell Signaling (#9271); Smad2, Cell Signaling (#5339S); phospho-Smad2, Cell Signaling (#3108S); HRP-linked sheep anti-mouse IgG, GE healthcare (NA931); HRP-linked donkey anti-rabbit IgG, GE healthcare (NA934).

#### 2.6. Dual-luciferase reporter assay

MCF10A cells were co-transfected with pRL-SV40 (Promega), 2  $\times$  DR5-tk/pGL3, which has two retinoic acid response elements, 2  $\times$  DR5 (kindly provided by Dr. Shigeaki Kato), and pMXs-RARA or pMXs-rara $\Delta$ 408-416 by calcium phosphate transfection; total DNA was equalized by the addition of empty vector. The day after transfection, extracts were harvested and assayed with the dual-luciferase reporter kit (Promega).

#### 2.7. Quantitative real-time PCR

Total RNA was extracted using Chomczynski's method (Chomczynski and Sacchi, 1987) or ISOGEN (NIPPON GENE) and incubated with reverse transcriptase SuperScript III

(Invitrogen) using random hexamers to obtain cDNA. Real-time PCR was performed by the StepOnePlus real-time PCR system (Applied Biosystems) using Taqman gene expression assays (Applied Biosystems) and Taqman gene expression master mix (Applied Biosystems). Quantification of relative mRNA expression levels was normalized to 18S ribosomal RNA. The following Taqman gene expression assays were used. SNAIL, Hs00195591\_m1; SLUG, Hs00950344\_m1; FOXC2, Hs00270951\_s1; ZEB1, Hs00232783\_m1; ZEB2, Hs00207691\_m1; TGFBR1, Hs00610320\_m1; TGFBR2, Hs00234253\_m1; TGFBI, Hs00998133\_m1; TGFBI2, Hs00234244\_m1; SMAD3, Hs00969210\_m; 18S, Hs99999901\_s1.

#### 2.8. Knockdown viral vectors

H1 promoter-driven ZEB1 knockdown vectors were constructed from an HIV-based SIN lentiviral vector (System biosciences), into which a puromycin resistance marker was introduced. An H1 promoter-driven ZEB2 knockdown vector was constructed from the pMXs retroviral vector bearing blasticidin resistance marker. Pairs of oligonucleotide sequences encoding shRNA are listed in Table S1.

### 3. Results

#### 3.1. Overexpression of RARA gene disrupted hollow lumen structures of 3D-cultured MCF10A mammary epithelial cells

To identify genes cooperating with ERBB2 in the early stages of breast cancer tumorigenesis under microenvironments mimicking that of the mammary gland, we first established an MCF10A clone suitable for 3D culture screening. To evaluate the capability of the clone to induce disruption of 3D structures, and to enable screening of genes cooperating with ERBB2, we introduced an oncogenic ERBB2 expression unit under the control of a tetracycline-responsive DNA element (MCF10A/Tet-on/TRE-ERBB2VE). We used a full-length ERBB2 mutant, ERBB2<sup>V659E</sup>, which forms homo- and heterodimers with other ERBB receptor family members and whose tyrosine kinase activity is constitutively activated (Yarden and Sliwkowski, 2001; Baselga and Swain, 2009). During the serial cloning steps, we chose the MCF10A clones most suitable for screening. When embedded in Matrigel, the MCF10A clone was required to show normal development of acinus structures without ERBB2VE induction (Figure S1B, Dox.(–) panel). Normal acinus had well-ordered spheroid structures and its inner area seemed to have a lower cell density. Then, the induction of ERBB2VE (Figure S1B, Dox.(+) panel) had to induce clear phenotypic changes including distorted luminal structures with high density of inner cells, “multi-acinar” morphology. To efficiently introduce target genes into human cells, we established an MCF10A clone expressing an ecotropic retroviral receptor (mSlc7a1) (MCF10A/Tet-on/TRE-ERBB2VE/Eco, Figure S1A).

We selected the 52 genes (51 genes plus wild type ERBB2) in the 17q12–21 amplicon and divided them into 10 subgroups consisting of five to six genes (Table S2). Each subgroup was introduced into the MCF10A/Tet-on/TRE-ERBB2VE/Eco cells

and cultured with or without doxycycline to examine the morphological changes induced by genes cooperating with *ERBB2VE* (Figure 1A, lower panels) or acting alone (upper panels) in the same cells, respectively. Albeit in the absence of *ERBB2VE* (Dox(-)), subgroup #3 showed remarkable filled luminal structures with larger spherical bodies (approximately 200  $\mu\text{m}$  in diameter) compared with the mock control (less than approximately 120  $\mu\text{m}$ ) and #10 showed aggregation (Figure 1B, S2). Subgroup #6 enhanced the aggregation by day

15 when *ERBB2VE* expression was induced at day 4 (Figure 1B, S2). We subsequently tested each of the 16 individual genes from these three subgroups, and found that the *RARA* gene from subgroup #3 caused similar aberrant structures in both the absence and presence of *ERBB2VE* (Figure 1C), as seen in the subgroup #3-infected cells. We did not detect any remarkable transforming activity in candidate genes included in both subgroup #6 and #10 using the method of evaluating the function of those alone (Supplementary file 2).

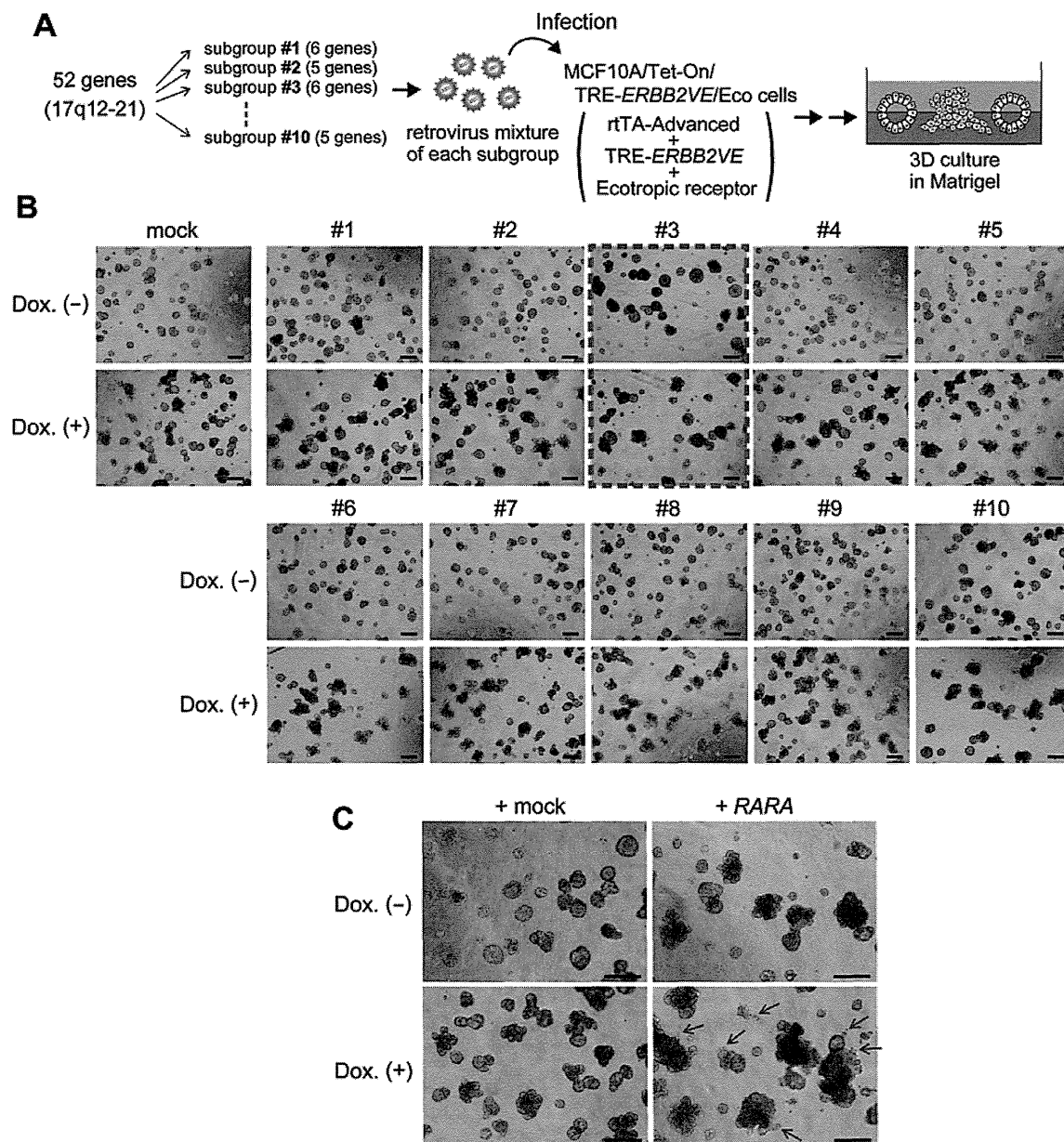


**Figure 1** – MCF10A 3D culture-based screening for genes coamplified with *ERBB2* and identification of *RARA* as a gene inducing filled-lumen structures. (A) Overview of the screening system. Fifty-two genes on the 17q12–21 amplicon including wild type *ERBB2* were selected as screening targets. We divided full-length cDNAs corresponding to those genes into ten subgroups and introduced them into MCF10A/Tet-on/TRE-*ERBB2VE*/Eco cells using retroviruses. The cells were embedded in Matrigel and allowed to proliferate. (B) Selection of transformed gene subgroups using a 3D culture system. Cells were infected with retrovirus mixture for each subgroup, embedded in Matrigel and cultured for 15 days. In the bottom panels, *ERBB2VE* was induced with Dox at day 4. Scale bars represent 200  $\mu\text{m}$ . Magnified pictures are provided in Figure S2. (C) Activity of *RARA* in both *ERBB2VE* (-) and (+) backgrounds. MCF10A/Tet-on/TRE-*ERBB2VE*/Eco cells were transfected with mock (left panels) or *RARA* (right panels) retroviruses and were cultured on Matrigel for 14 days. In the right panels, *ERBB2VE* was induced by the addition of Dox at day 4. Arrows indicate raptured structures. Scale bars represent 200  $\mu\text{m}$ .

### 3.2. Overexpression of RARA induced invasive transformation in Matrigel-containing collagen I cultures

Coexpression of RARA and ERBB2VE led to the formation of larger cell clusters with a slightly protrusive outgrowth (Figure 1C), raising the possibility that RARA conferred migratory or invasive activities to MCF10A cells. To test this hypothesis, we cultured RARA-expressing cells in collagen I-containing Matrigel, as previously performed, to assess the invasiveness of MCF10A cells (Seton-Rogers et al., 2004). Intriguingly, we noticed that the MCF10A cells overexpressing RARA displayed a lattice-like network of invasive projections in the Matrigel-collagen I mixture, while those expressing ERBB2VE alone did not (Figure 2A). This response of RARA-expressing cells was dependent on the multiplicity of infection (MOI) of retroviruses, whereas control virus did not induce such response (Figure 2B and C). In addition, coexpression of both RARA and ERBB2VE resulted in thicker cords containing multiple acini-like structures (Figure 2A). These results suggest that RARA is a potent invasion-associated gene that is qualitatively different from ERBB2VE, which is an inducer of acinar expansion without invasion into the surrounding matrix.

RAR $\alpha$ , which is encoded by RARA, is a nuclear receptor for retinoic acid and functions as a transcriptional regulator for genes involving multicellular development, differentiation, and apoptosis. In the absence of ligand or in the presence of antagonists, target genes are silenced due to the binding of co-repressors (CoRs) to RAR $\alpha$ . Binding of RAR $\alpha$  agonists to the ligand binding pocket induces allosteric changes in the ligand binding domain (LBD), leading to the movement of the C-terminal helix H12, which then generates a novel interaction surface for coactivators (CoAs) (Bastien and Rochette-Egly, 2004; Altucci and Gronemeyer, 2001). In a previous study, it was demonstrated that deletion of H12 increases CoR-binding and results in the repression of gene expression (Farboud et al., 2003). To examine the role of the transcriptional activity of RAR $\alpha$  for the invasive protrusion phenotype, we constructed a RAR $\alpha$  deletion mutant (RAR $\alpha$  $\Delta$ 408–416) lacking the H12 motif. In a retinoic acid response element (RARE)-Luc reporter assay, the wild type RAR $\alpha$  enhanced luciferase activity in a dose-dependent manner whereas the RAR $\alpha$  $\Delta$ 408–416 mutant rather suppressed it (Figure S3A). When we introduced retrovirus for the mutant at the same MOI as the wild type, MCF10A cells expressing RAR $\alpha$  $\Delta$ 408–416 did not form protrusions in the Matrigel and collagen I culture (Figure S3B). Thus, it is likely that the transcriptional activation by RAR $\alpha$ , not the transcriptional repression in cooperation with CoR, is required for the invasive phenotype in cells. The dominant negative activity of RAR $\alpha$  $\Delta$ 408–416 likely resulted from an antagonistic role against intrinsically activated endogenous RAR proteins, which is insufficient to cause transformation.

### 3.3. RARA induced EMT-related gene signatures

In 2D cultures, we observed that MCF10A cells overexpressing RARA displayed a fibroblast-like morphology, whereas control mock-infected cells grew in well-ordered epithelial clusters (Figure 3A), suggesting that RARA acts as an EMT-inducing

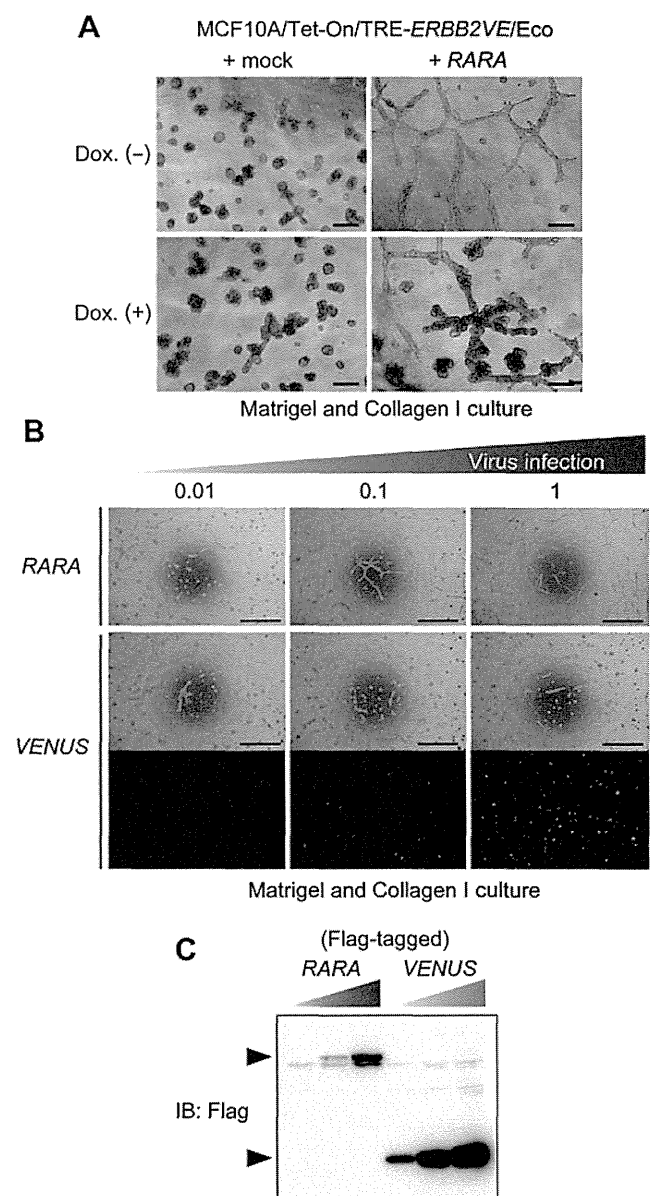


**Figure 2** – RARA-induced invasive transformation in Matrigel containing collagen I in a manner dependent on its expression levels. (A) Identification of an invasive phenotype induced by RARA in Matrigel and collagen I culture. MCF10A/Tet-on/TRE-ERBB2VE/Eco cells overexpressing RARA were cultured in a 1:1 mixture of Matrigel and collagen I for 11 days. ERBB2VE was induced by the addition of Dox at day 4. Scale bars represent 200  $\mu$ m. (B) Detection of dose-dependent RARA activity. MCF10A/Tet-on/TRE-ERBB2VE/Eco cells were infected with retroviruses containing RARA or Venus with Flag epitope tag at the indicated MOIs. Cells were grown in a 1:2 mixture of Matrigel and Collagen I for 4 days in the absence of Dox. Scale bars represent 1 mm. (C) MOIs-related expression levels. Protein levels in the cells used in (B) were analyzed by immunoblotting using the antibody against Flag. The upper band indicates the expression of RAR $\alpha$ , and the lower band indicates that of Venus.

factor. To address this hypothesis, we examined the expression of epithelial and mesenchymal markers by immunoblotting. In MCF10A cells expressing RARA, the epithelial marker E-cadherin was downregulated, whereas mesenchymal

markers N-cadherin and vimentin were upregulated (Figure 3B). These changes in E-cadherin and N-cadherin expression were totally abrogated by the mutant *rara* $\Delta$ 408–416 (Figure S3C), suggesting that RARA induces EMT in MCF10A cells via RAR $\alpha$ -mediated transcriptional activation. In contrast, *ERBB2VE* did not affect the epithelial morphology in monolayer cultures nor the expression of EMT markers (Figure 3B). N-cadherin upregulation by RARA was also seen in MDA-MB-361 breast cancer cells (Figure S3D).

To examine whether the expression levels of EMT-related genes were regulated by RARA, we performed real-time PCR analysis. RARA-overexpressing MCF10A cells exhibited approximately 4-, 2.5-, and 12-fold increases at day 4 in the mRNA levels of the *SLUG*, *FOXC2*, and *ZEB* gene families, respectively, compared with control MCF10A cells. Also, the mRNA levels of *TGFBR1*, *TGFBR2*, *TGFB2*, and *SMAD3* increased by 4-, 2.5-, 7-, and 2.5-fold, respectively, at day 4 in RARA-overexpressing MCF10A cells (Figure 3C). Time-course experiments revealed that changes in E-cadherin and N-cadherin occurred after 24 h of RARA induction (Figure S4), suggesting that transcriptional cascades involving EMT-inducing factors are activated during this time period. These results suggest that RAR $\alpha$  activates the

EMT signaling program before inducing a protrusive behavior in 3D cultures with collagen I.

Because RARA induced upregulation of key factors involved in the TGF- $\beta$ /SMAD signaling pathway (Figure 3C), we hypothesized that RARA activated this pathway and then induced invasion in 3D cultures as well as EMT. Therefore, we examined whether the inhibition of the TGF- $\beta$ /SMAD pathway suppressed phenotypic changes in RARA-expressing MCF10A cells. Optimal concentration of an inhibitor of the TGF- $\beta$  receptor type I, SB-431542 (Figure S5A), partially suppressed changes in the expression levels of EMT markers (Figure S5B) and protrusion (Figure S5C). These results suggest that the TGF- $\beta$  signaling pathway is partially responsible for EMT and invasion caused by RARA. We subsequently examined whether the activation of the TGF- $\beta$  pathway was sufficient to induce such changes. Stimulation of parental MCF10A cells with TGF- $\beta$ 1 led to both slight downregulation of E-cadherin and upregulation of N-cadherin (Figure S5D). Also, modest effects on the phenotype were observed in 3D cultures using Matrigel and collagen I (Figure S5E), consistent with the previous result showing that the expression of TGF- $\beta$ 1 without the activation of *ERBB2* hardly displayed any invasive activity (Seton-Rogers et al., 2004). These results suggest

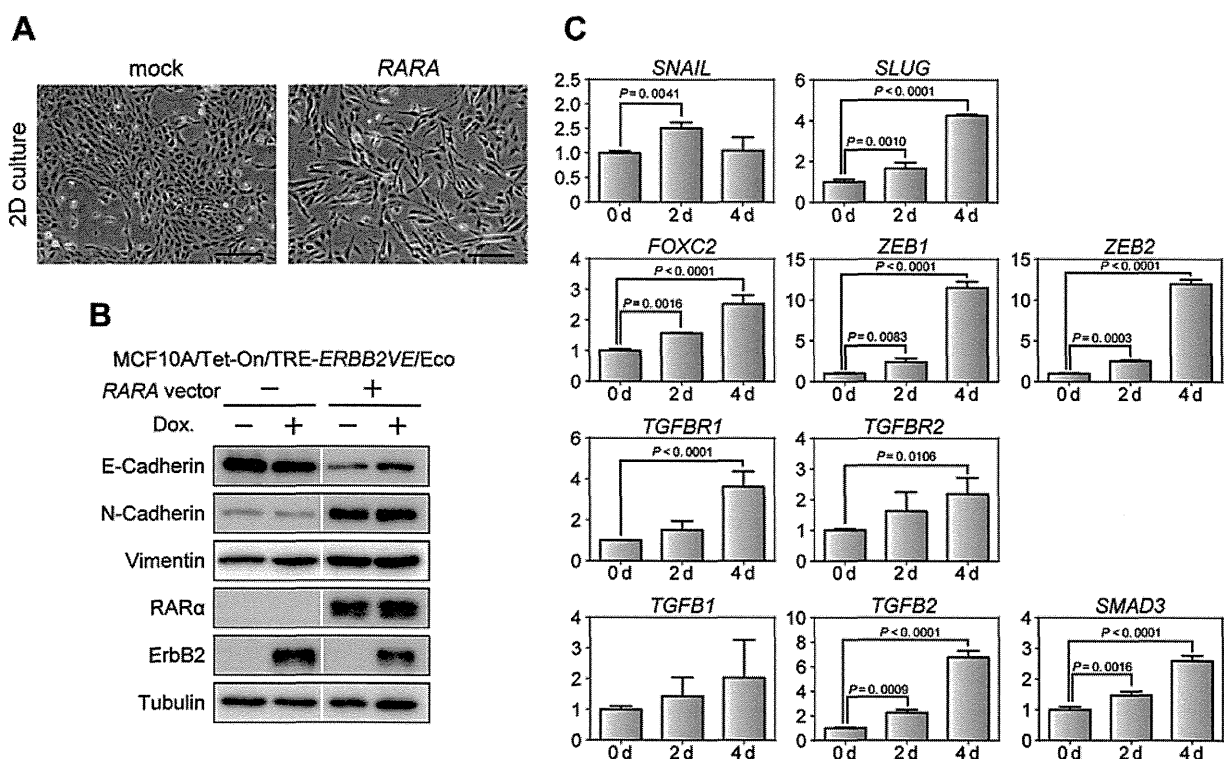


**Figure 3** – Induction of EMT-like morphological changes and upregulation of EMT-related genes by RARA overexpression. (A) Mesenchymal-like transition induced by RARA. MCF10A/Tet-on/TRE-ERBB2VE/Eco cells overexpressing the indicated genes exhibited different morphologies in 2D culture. Scale bars represent 200  $\mu$ m. (B) Expression analyses for EMT markers. The expression levels of the indicated proteins were analyzed by immunoblotting. Tubulin was used as a loading control. To evaluate effects of *ERBB2VE*, Dox-treated samples for 2 days (Dox (+) lanes) were simultaneously evaluated, but revealed to be negligible compared with the effects by RARA. White line, trimmed margin of unrelated sample lanes. (C) Quantitative analyses of mRNA changes induced by RARA. The mRNA expression levels of the indicated genes were measured by real-time PCR. MCF10A/Tet-on cells were infected with lentiviruses for TRE-RARA (MCF10A/Tet-on/TRE-RARA), and RNA was extracted at the indicated days after Dox addition. Real-time PCR values were normalized to the internal control, 18S ribosomal RNA. The y-axis depicts the fold-change in each normalized mRNA compared with Dox (-) cells (0 d). The represented data are shown as mean  $\pm$  s.d.. Dunnett's multiple comparisons test were performed to assess statistical significance.